Article

Hierarchical Assembly of Helicate-Type Dinuclear Titanium(IV) Complexes

Markus Albrecht, Sebastian Mirtschin, Marita de Groot, Ingo Janser, Jan Runsink, Gerhard Raabe, Michael Kogej, Christoph A. Schalley, and Roland Frhlich

J. Am. Chem. Soc., **2005**, 127 (29), 10371-10387• DOI: 10.1021/ja052326j • Publication Date (Web): 28 June 2005

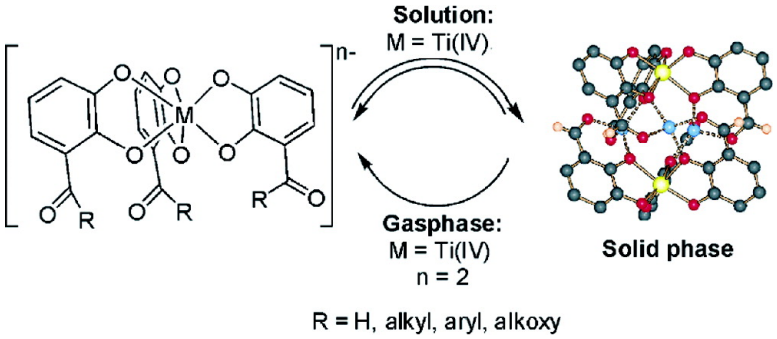

More About This Article

Additional resources and features associated with this article are available within the HTML version:

- Supporting Information
- Links to the 11 articles that cite this article, as of the time of this article download
- Access to high resolution figures
- Links to articles and content related to this article
- Copyright permission to reproduce figures and/or text from this article

View the Full Text HTML

J|A|C|S
ARTICLES
Published on Web 06/28/2005

Hierarchical Assembly of Helicate-Type Dinuclear Titanium(IV) Complexes

Markus Albrecht,*,† Sebastian Mirtschin,† Marita de Groot,† Ingo Janser,† Jan Runsink,† Gerhard Raabe,† Michael Kogej,‡ Christoph A. Schalley,*,‡ and Roland Fröhlich§

Contribution from the Institut für Organische Chemie, RWTH Aachen, Landoltweg 1, 52074 Aachen, Germany, Kekulé-Institut für Organische Chemie und Biochemie, Universität Bonn, Gerhard-Domagk-Strasse 1, 53121 Bonn, Germany, and Organisch-Chemisches Institut, Universität Münster, Corrensstrasse 40, 48149 Münster, Germany

Received April 11, 2005; E-mail: markus.albrecht@oc.rwth-aachen.de; c.schalley@uni-bonn.de

Abstract: The ligands **4**−**7-H**$_2$ were used in coordination studies with titanium(IV) and gallium(III) ions to obtain dimeric complexes $Li_4[(\mathbf{4}-\mathbf{7})_6Ti_2]$ and $Li_6[(\mathbf{4/5a})_6Ga_2]$. The X-ray crystal structures of $Li_4[(\mathbf{4})_6Ti_2]$, $Li_4[(\mathbf{5b})_6Ti_2]$, and $Li_4[(\mathbf{7a})_6Ti_2]$ could be obtained. While these complexes are triply lithium-bridged dimers in the solid state, a monomer/dimer equilibrium is observed in solution by NMR spectroscopy and ESI FT-ICR MS. The stability of the dimer is enhanced by high negative charges (Ti(IV) versus Ga(III)) of the monomers, when the carbonyl units are good donors (aldehydes versus ketones and esters), when the solvent does not efficiently solvate the bridging lithium ions (DMSO versus acetone), and when sterical hindrance is minimized (methyl versus primary and secondary carbon substituents). The dimer is thermodynamically favored by enthalpy as well as entropy. ESI FT-ICR mass spectrometry provides detailed insight into the mechanisms with which monomeric triscatecholate complexes as well as single catechol ligands exchange in the dimers. Tandem mass spectrometric experiments in the gas phase show the dimers to decompose either in a symmetric (Ti) or in an unsymmetric (Ga) fashion when collisionally activated. The differences between the Ti and Ga complexes can be attributed to different electronic properties and a charge-controlled reactivity of the ions in the gas phase. The complexes represent an excellent example for hierarchical self-assembly, in which two different noncovalent interactions of well balanced strengths bring together eleven individual components into one well-defined aggregate.

Introduction

Self-assembly of suitably programmed building blocks is ubiquitous in nature[1] and often occurs on several hierarchy levels simultaneously in order to generate functional systems. For example, the shell-forming protein building blocks of the tobacco mosaic virus[2] need to fold into the correct tertiary protein structure before they can be organized around a templating RNA strand. All these processes are mediated by noncovalent forces which guide the formation of secondary structure elements on the lowest hierarchy level. These form the tertiary structure on the next level which displays the necessary binding sites for the assembly of the virus from a total of 2131 building blocks to occur as programmed on the highest level. Other examples for hierarchical self-assembly are multienzyme complexes, the formation of cell membranes with all the receptors, ion channels, or other functional entities embedded into them, or molecular motors such as ATP synthase. Self-assembly is thus an efficient strategy to create complexity and, together with it, function in nature.

Self-assembly[3] often also plays a crucial role for the specific formation of well-defined, artificial supramolecular species.[4] However, aggregation, which is based on solely one type of interaction between the components, can only develop limited complexity. For the generation of a higher degree of complexity, as it is found in nature's functional molecules, different noncovalent interactions[5] are required, which have different but well-balanced relative strengths. On one hand, using self-assembly strategies on several different levels of hierarchy makes the programming of the individual components more challenging for the synthetic chemist. On the other hand, hierarchical self-assembly promises to simplify the creation of complexity.[6] A precise understanding of the properties of such systems is a prerequisite for any design strategy.

† RWTH Aachen.
‡ Universität Bonn.
§ Universität Münster.

(1) Hamilton, T. D.; MacGillivray, L. R. In *Self-Assembly in Biochemistry*; Atwood, J. L.; Steed, J. W., Eds.; Encyclopedia of Supramolecular Chemistry; Dekker: New York, 2004; pp 1257−1262.
(2) Klug, A. *Angew. Chem.* **1983**, *95*, 579−596; *Angew. Chem., Int. Ed. Engl.* **1983**, *22*, 565−582.
(3) For example, see: (a) Lindsey, J. S. *New J. Chem.* **1991**, *15*, 153−180. (b) Whitesides, G. M.; Mathias, J. P.; Seto, C. T. *Science* **1991**, *254*, 1312−1319. (c) Philp, D.; Stoddart, J. F. *Angew. Chem.* **1996**, *108*, 1243−1286; *Angew. Chem., Int. Ed. Engl.* **1996**, *35*, 1154−1196. (d) Schalley, C. A.; Lützen, A.; Albrecht, M. *Chem.—Eur. J.* **2004**, *10*, 1072−1080.
(4) (a) Lehn, J. M. *Struct. Bonding* **1973**, *16*, 1−69. (b) Lehn, J.-M. *Supramolecular Chemistry*; VCH: Weinheim, 1995. (c) Vögtle, F. *Supramolekulare Chemie*; Teubner: Stuttgart, 1992. (d) Steed, J. W.; Atwood, J. L. *Supramolecular Chemistry*; Wiley: Chichester, 2000.
(5) For example, see: Greig, L. M.; Philp, D. *Chem. Soc. Rev.* **2001**, *30*, 287−302.

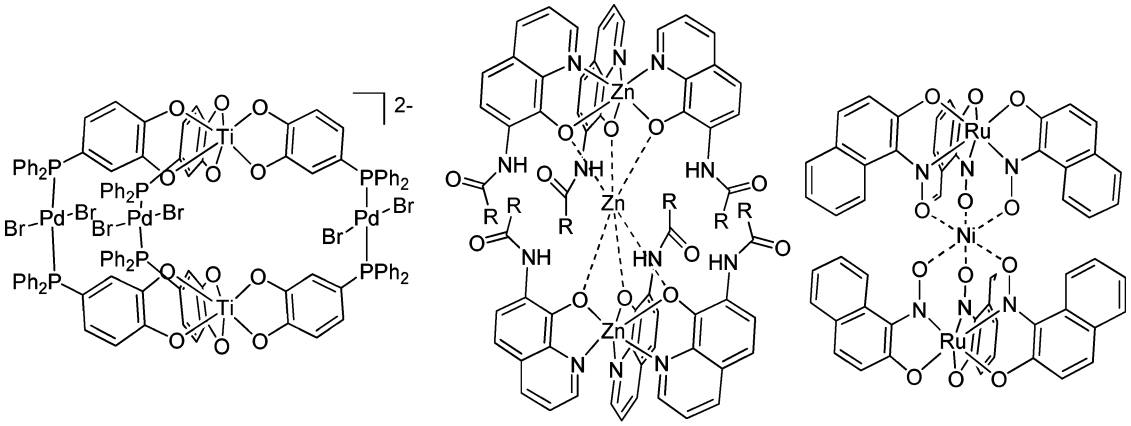

1 2 3

Figure 1. Helicate-type complexes formed by hierarchical self-assembly.

Helicates[7] are a class of very simple metallosupramolecular compounds which allowed the chemists to investigate basic aspects of supramolecular chemistry,[8] such as stereochemistry,[9] regiochemistry,[10] or the mechanisms of self-assembly.[11] Only very few examples can be found, in which helicates are formed by hierarchical self-assembly. Hannon[12] and Nitschke[13] describe the in situ formation of dinuclear helicates by imine condensation of diamines with pyridinyl-2-carbaldehydes in the presence of appropriate metal ions. Both metal coordination and imine condensation are reversible, thermodynamically controlled processes which finally give rise to the helicate products in a one-pot hierarchical process.[14]

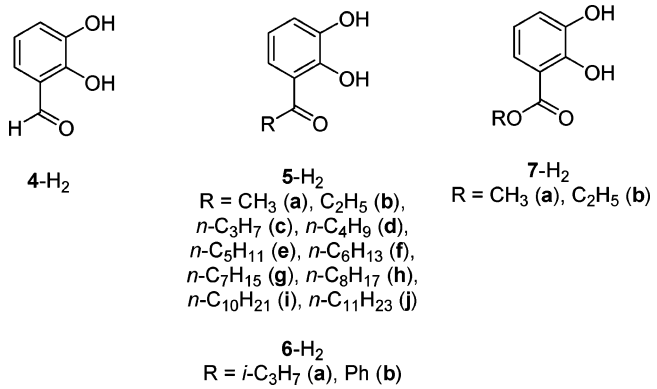

4-H_2

5-H_2
R = CH_3 (**a**), C_2H_5 (**b**), n-C_3H_7 (**c**), n-C_4H_9 (**d**), n-C_5H_{11} (**e**), n-C_6H_{13} (**f**), n-C_7H_{15} (**g**), n-C_8H_{17} (**h**), n-$C_{10}H_{21}$ (**i**), n-$C_{11}H_{23}$ (**j**)

6-H_2
R = i-C_3H_7 (**a**), Ph (**b**)

7-H_2
R = CH_3 (**a**), C_2H_5 (**b**)

Figure 2. Ligands described in this study.

Complexes **1**,[15] **2**,[16] and **3**[17] represent examples for helicate-type complexes which are formed by two different metal binding events. In principle, mononuclear tris-ligand complexes are formed which are then connected by three (**1**) or one metal ion (**2,3**), respectively. Finally, the helicate-type compounds are obtained (Figure 1).

In this paper, we present the lithium-controlled hierarchical assembly of a series of dinuclear helicate-type titanium(IV) and gallium(III) complexes with catecholate ligands,[18] which bear aldehyde (**4**-H_2), ketone (**5a**−**j**-H_2, **6a,b**-H_2), or ester functions (**7a,b**-H_2) in the 3-position of the catechol (Figure 2). The properties of these complexes are studied in the solid state, in solution, and in the gas phase.

Results and Discussion

Ligand Synthesis. Aldehyde **4**-H_2 is commercially available while the ligands **5**−**7**-H_2 were prepared as outlined in Scheme

(6) Selected examples: (a) Percec, V.; Cho, W.-D.; Ungar, G.; Yeardley, D. J. P. *Angew. Chem.* **2000**, *112*, 1662−1666; *Angew. Chem., Int. Ed.* **2000**, *39*, 1597−1602. (b) Elemans, J. A. A. W.; Rowan, A. E.; Nolte, R. J. M. *J. Mater. Chem.* **2003**, *13*, 2661−2670. (c) Würthner, F.; Yao, S.; Beginn, U. *Angew. Chem.* **2003**, *115*, 3368−3371; *Angew. Chem., Int. Ed* **2003**, *42*, 3247−3250. (d) Elemans, J. A. A. W.; Rowan, A. E.; Nolte, R. J. M. *J. Am. Chem. Soc.* **2002**, *124*, 1532−1540. (e) Berl, V.; Krische, M. J.; Huc, I.; Lehn, J.-M.; Schmutz, M. *Chem.*−*Eur. J.* **2000**, *6*, 1938−1946. (f) Kawasaki, T.; Tokuhiro, M.; Kimizuka, N.; Kunitake, T. *J. Am. Chem. Soc.* **2001**, *123*, 6792−6800. (g) Ikkala, O.; ten Brinke, G. *Chem. Commun.* **2004**, 2131−2137.

(7) (a) Lehn, J.-M.; Rigault, A.; Siegel, J.; Harrowfield, J.; Chevrier, B.; Moras, D. *Proc. Natl. Acad. Sci. U.S.A.* **1987**, *84*, 2565−2569. For other early examples, see: (b) Scarrow, R. C.; White, D. L.; Raymond, K. N. *J. Am. Chem. Soc.* **1985**, *107*, 6540−6546. (c) Lehn, J.-M.; Rigault, A. *Angew. Chem.* **1988**, *100*, 1121−1122; *Angew. Chem., Int. Ed. Engl.* **1988**, *27*, 1095−1097. (d) Constable, E. C.; Elder, S. M.; Healy, J.; Ward, M. D.; Tocher, D. A. *J. Am. Chem. Soc.* **1990**, *112*, 4590−4592. (e) Williams, A. F.; Piguet, C.; Bernardinelli, G. *Angew. Chem.* **1991**, *103*, 1530−1532; *Angew. Chem., Int. Ed. Engl.* **1991**, *30*, 1490−1492. (f) Bernardinelli, G.; Piguet, C.; Williams, A. F. *Angew. Chem.* **1992**, *104*, 1662−1664; *Angew. Chem., Int. Ed. Engl.* **1992**, *31*, 1622−1624. (g) Saalfrank, R. W.; Seitz, V.; Caulder, D.; Raymond, K. N.; Teichert, M.; Stalke, D. *Eur. J. Inorg. Chem.* **1998**, 1313−1317.

(8) Reviews: (a) Constable, E. C. *Tetrahedron* **1992**, *48*, 10013−10059. (b) Piguet, C.; Bernardinelli, G.; Hopfgartner, G. *Chem. Rev.* **1997**, *97*, 2005−2062. (c) Albrecht, M. *Chem. Rev.* **2001**, *101*, 3457−3498. (d) Hannon, M. J.; Childs, L. J. *Supramol. Chem.* **2004**, *16*, 7−22. (e) Albrecht, M.; Janser, I.; Fröhlich, R. *Chem. Commun.* **2005**, 157−165. (f) See also: Saalfrank, R. W.; Demleitner, B. In *Transition Metals in Supramolecular Chemistry*; Sauvage, J.-P., Ed.; John Wiley & Sons: New York, 1999; Vol. 5, pp 1−51.

(9) Albrecht, M. *Chem.*−*Eur. J.* **2000**, *6*, 3485−3489.

(10) Piguet, C.; Hopfgartner, G.; Bocquet, B.; Schaad, O.; Williams, A. F. *J. Am. Chem. Soc.* **1994**, *116*, 9092−9102.

(11) (a) Pfeil, A.; Lehn, J.-M. *J. Chem. Soc., Chem. Commun.* **1992**, 838−840. (b) Albrecht, M. *Top. Curr. Chem.* **2004**, *248*, 105−139.

(12) (a) Childs, L. J.; Alcock, N. W.; Hannon, M. J. *Angew. Chem.* **2002**, *114*, 4418−4421; *Angew. Chem., Int. Ed.* **2002**, *41*, 4244−4247. (b) Hamblin, J.; Childs, L. J.; Alcock, N. W.; Hannon, M. J. *J. Chem. Soc., Dalton Trans.* **2002**, 164−169.

(13) Nitschke, J. R.; Schultz, D.; Bernardinelli, G.; Gérard, D. *J. Am. Chem. Soc.* **2004**, *126*, 16538−16543.

(14) See also: (a) Nitschke, J. R.; Lehn, J.-M. *Proc. Natl. Acad. Sci. U.S.A.* **2003**, *100*, 11970−11974. (b) Nitschke, J. R.; Hutin, M.; Bernardinelli, G. *Angew. Chem.* **2004**, *116*, 6892−6895; *Angew. Chem., Int. Ed.* **2004**, *43*, 6724−6727.

(15) (a) Sun, X.; Darren, W. J.; Caulder, D.; Powers, R. E.; Raymond, K. N.; Wong, E. H. *Angew. Chem.* **1999**, *111*, 1386-1390; *Angew. Chem., Int. Ed.* **1999**, *38*, 1303−1306. (b) Sun, X.; Johnson, D. W.; Caulder, D.; Raymond, K. N.; Wong, E. H. *J. Am. Chem. Soc.* **2001**, *123*, 2752−2763. (c) Sun, X.; Johnson, D. W.; Raymond, K. N.; Wong, E. H. *Inorg. Chem.* **2001**, *40*, 4504−4506.

(16) (a) Albrecht, M.; Witt, K.; Röttele, H.; Fröhlich, R. *Chem. Commun.* **2001**, 1330−1331. (b) Albrecht, M.; Witt, K.; Weis, P.; Wegelius, E.; Rissanen, K.; Fröhlich, R. *Inorg. Chim. Acta* **2002**, 25−32.

(17) (a) Das, A. K.; Rueda, A.; Falvello, L. R.; Peng, S.-M.; Batthacharya, S. *Inorg. Chem.* **1999**, *38*, 4365−4368. (b) For a related recent example, see: Heinicke, J.; Peulecke, N.; Karaghiosoff, K.; Mayer, P. *Inorg. Chem.* **2005**, *44*, 2137−2139.

(18) For triscatecholate complexes of titanium(IV) and gallium(III), see: (a) Borgias, B. A.; Cooper, S. R.; Koh, Y. B.; Raymond, K. N. *Inorg. Chem.* **1984**, *23*, 1009−1016. (b) Borgias, B. A.; Barclay, S. J.; Raymond, K. N. *J. Coord. Chem.* **1986**, *15*, 109−123.

Scheme 1. Preparation of the Ligands **5**−**7**-H_2

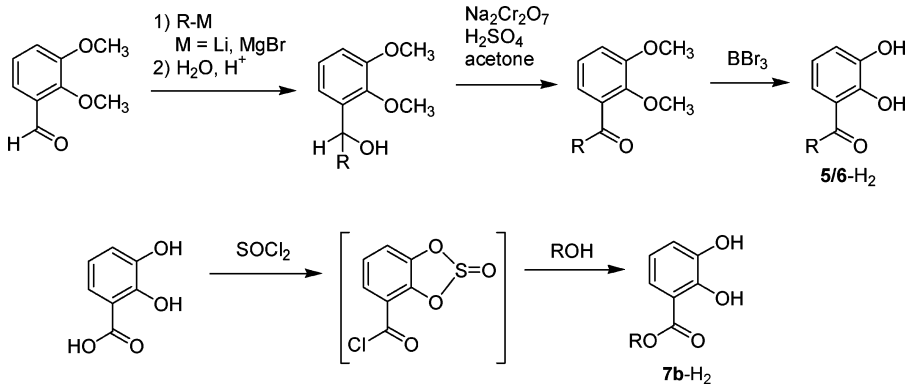

Scheme 2. Hierarchical Assembly of a Triply Lithium-Bridged Helicate-Type Complex

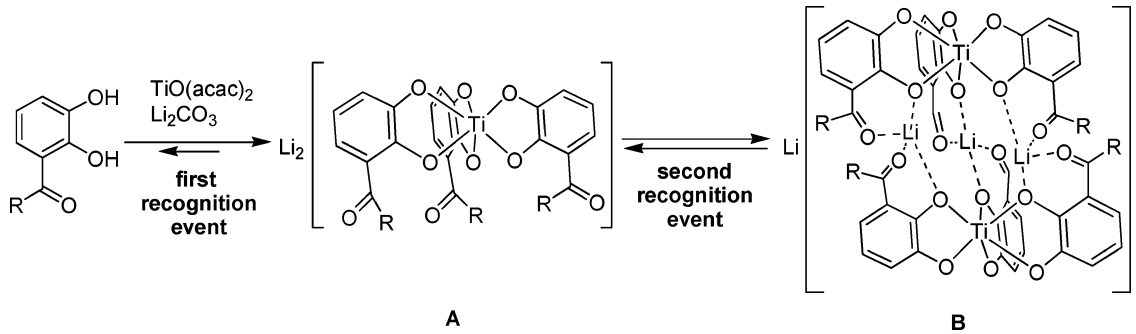

1. The ketones **5/6**-H_2 were obtained by addition of organolithium or Grignard reagents to 2,3-dimethoxybenzaldehyde, followed by Jones oxidation[19] and subsequent BBr_3 cleavage of the methyl ethers.[20] The initially prepared secondary alcohols were oxidized without purification.[21]

7a-H_2 was prepared by acidic esterification of 2,3-dihydroxybenzoic acid with methanol.[22] The synthesis of the ester **7b**-H_2 followed Raymond's procedure to generate the acid chloride of 2,3-dihydroxybenzoic acid[23] followed by in situ quenching with the alcohol.

Coordination Studies. The metal complexes "$Li_2[(\mathbf{4}-\mathbf{7})_3Ti]$" were prepared by dissolving 3 equiv of the corresponding ligand and 1 equiv of $TiO(acac)_2$ and Li_2CO_3 in DMF. After stirring overnight, the solvent is removed at 70 °C in vacuo to obtain the complexes in quantitative yield (Scheme 2).

The formation of mononuclear titanium(IV) complexes[18] **A** ($Li_2[(\mathbf{4}-\mathbf{7})_3Ti]$) corresponds to the first molecular recognition event. Due to the carbonyl donors at the ligands, lithium ions can be bound in a second recognition event, and triply bridged dinuclear helicate-type complexes **B** ($Li[(\mu\text{-}Li)_3\{(\mathbf{4}-\mathbf{7})_3Ti\}_2]$) are formed.[24] Monomer **A** and dimer **B** are observed in solution as well as in the gas phase. In the crystal, however, we only find the dimeric species **B** (vide infra). It should be noted that two isomers of monomer **A** can be formed, one of which has a facial or all-syn arrangement of the carbonyl groups and another one where one of them points to the opposite side of the complex in a meridional fashion. Upon aggregation the meridional isomer should lead to polymeric material, which is not observed. The coordination of Li^+ mediating dimer formation acts as a template for the formation of the facial geometry within the monomers at the same time. This is an example for the recursive effects that may occur in hierarchical self-assembly: The second assembly step influences the first one, and both are not independent from each other. The facial and meridional isomers of the monomeric complexes are in a dynamic equilibrium, undergoing an associative bailar twist rearrangement.[25] In the dimerization process this equilibrium is shifted toward the facial arrangement.

For comparison with the Ti complexes, the compounds "$Li_3[(\mathbf{4})_3Ga]$" and "$Li_3[(\mathbf{5a})_3Ga]$" were made in DMF from 3 equiv of **4**-H_2 or **5a**-H_2 and $Ga(acac)_3$. Here, the monomer $Li_3[(\mathbf{4/5a})_3Ga]$ and the dimer $Li_3[(\mu\text{-}Li)_3\{(\mathbf{4/5a})_3Ga\}_2]$ are observed as well.

The formation of dimers in an equilibrium with the corresponding monomers is highly specific for lithium counterions. Ions such as Na^+ or K^+ with their larger ionic radii did not mediate dimer formation according to the absence of any indication for their formation in the NMR and ESI MS spectra.[26] This effect is likely due to an almost perfect fit of the Li^+ ions inside the three pockets formed upon dimerization, while Na^+ and K^+ do not fit due to their larger spatial demand and the preference for a higher coordination number. Therefore probably mixtures of facial and meridional isomers are formed with those cations.

(19) Brown, H. C.; Garg, C. P.; Liu, K.-T. *J. Org. Chem.* **1971**, *36*, 387−390.
(20) McOmie, J. F. W.; West, D. E. *Org. Synth. Collect. Vol. V* **1973**, 412−414.
(21) The synthesis follows a procedure described in: Awad, W. L.; El-Neweihy, M. F.; Selim, S. F. *J. Org. Chem.* **1958**, *23*, 1783−1784.
(22) Sharma, S. K.; Miller, M. J.; Payne, S. M. *J. Med. Chem.* **1989**, *32*, 357−367.
(23) Gramer, C. J.; Raymond, K. N. *Org. Lett.* **2001**, *3*, 2827−2830.
(24) For dinuclear helicate-type titanium(IV) complexes with three coordinated lithium cations, see: Albrecht, M.; Kotila, S. *Chem. Commun.* **1996**, 2309−2310.
(25) Meyer, M.; Kersting, B.; Powers, R. E.; Raymond, K. N. *Inorg. Chem.* **1997**, *36*, 5179−5191.
(26) For examples of templating in the formation of helicates, see: (a) Albrecht, M.; Blau, O.; Fröhlich, R. *Chem.—Eur. J.* **1999**, *5*, 48−56. (b) Albrecht, M.; Blau, O.; Fröhlich, R. *Proc. Natl. Acad. Sci. U.S.A.* **2002**, *99*, 4876−4882.

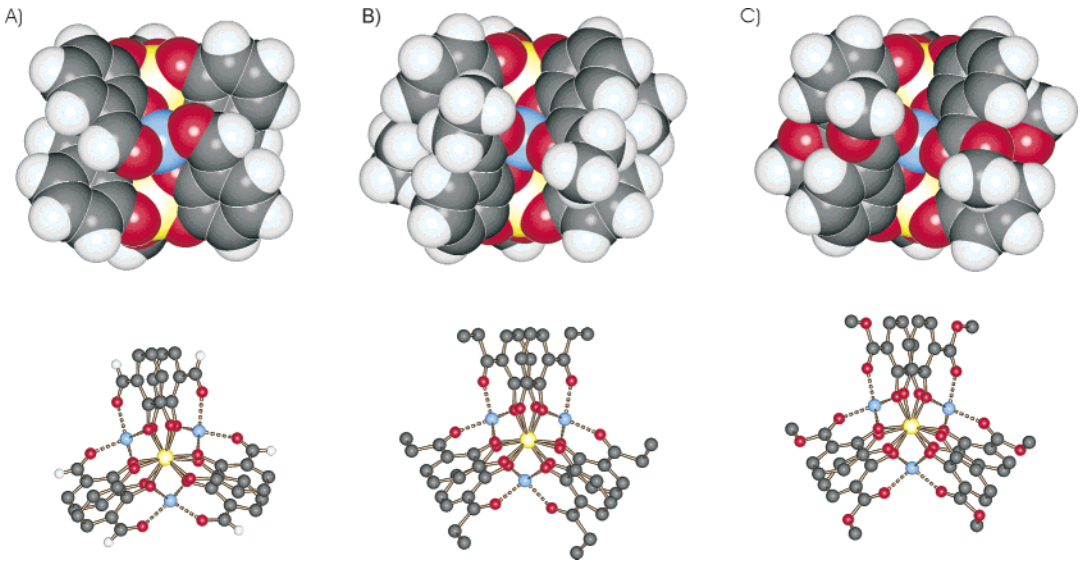

Figure 3. Solid-state structures of the monoanions $[Li_3(\mathbf{4})_6Ti_2]^-$ (A), $[Li_3(\mathbf{5b})_6Ti_2]^-$ (B), and $[Li_3(\mathbf{7a})_6Ti_2]^-$ (C). Side view (top) and view along the Ti−Ti axis (bottom; hydrogens (except at the aldehyde) are omitted).

X-ray Crystal Structures. $Li_2[(\mathbf{4})_3Ti]$, $Li_2[(\mathbf{5b})_3Ti]$, and $Li_2[(\mathbf{7a})_3Ti]$ were crystallized from DMF/diethyl ether to obtain red crystals suitable for X-ray crystallography. X-ray crystal structure analyses revealed the complexes to exist as dimers in the solid state (Figure 3). Due to the poor quality of the crystal of $Li_4[(\mathbf{5b})_6Ti_2]$, only a low-quality structure could be obtained for this compound. Nevertheless, it unambiguously confirms its dimeric nature.

In $Li_4[(\mathbf{4})_6Ti_2]$, two triscatecholate titanium(IV) complex units are formed with the aldehydes of the ligands **4** all orientated in the same direction (facial arrangement). Three pseudo-tetrahedrally coordinated lithium cations are bridging two of the $[(\mathbf{4})_3Ti]^{2-}$ moieties by binding to an internal catecholate oxygen (in 2-position) and a carbonyl oxygen atom of each Ti-complex moiety.

The structure of $[Li_3(\mathbf{4})_6Ti_2]^-$ can formally be regarded as a triple-stranded dinuclear helicate with three lithium containing "noncovalent" ligands $[\mathbf{4}\text{-Li-}\mathbf{4}]^{3-}$. As stated above, the formation of this noncovalent helicate needs to be considered as a true eleven-component self-assembly process (6 × **4**, 3 × Li, 2 × Ti) with two different kinds of recognition events: one between titanium(IV) and catecholate and the other between Li^+ and the salicylaldehyde units.

The structures of $Li_4[(\mathbf{5b})_6Ti_2]$ and $Li_4[(\mathbf{7a})_6Ti_2]$ are very similar to the one of the complex of ligand **4**. From the representation in Figure 3 (B, C), the orientation of the ethyl or methoxy substituents in the clefts of the triple-stranded helical structure can be nicely seen. The sizes of the three dimer structures are very similar with Ti−Ti distances of 5.522 Å ($Li_4[(\mathbf{4})_6Ti_2]$), 5.535 Å ($Li_4[(\mathbf{5b})_6Ti_2]$), or 5.474 Å ($Li_4[(\mathbf{7a})_6Ti_2]$).

The averaged Li−O distances are found to be 1.937 Å ($Li_4[(\mathbf{4})_6Ti_2]$), 1.933 Å ($Li_4[(\mathbf{5b})_6Ti_2]$), or 1.918 Å ($Li_4[(\mathbf{6a})_6Ti_2]$). The shortening of these interactions from the aldehyde to the ketone to the ester represents the increasing donor strengths of the differently substituted carbonyl groups.

Solution Studies: NMR Spectroscopy. ^{1}H NMR investigations of the complexes reveal the presence of dimer/monomer equilibria in solution. The monomer/dimer ratio strongly depends on the lithium coordinating ability of the solvent, and thus different ratios are observed in different solvents.

DMSO-d_6 as a solvent is strongly competing with the catecholate complexes for the Li^+ ions and therefore destabilizes the dimers.[27] For the aldehyde derivative "$Li_2[(\mathbf{4})_3Ti]$", only ^{1}H NMR signals of monomeric $Li_2[(\mathbf{4})_3Ti]$ are observed in DMSO-d_6 at δ (ppm) = 10.09 (s), 6.69 (dd, J = 7.4, 1.3 Hz), 6.36 (t, J = 7.4 Hz), and 6.23 (dd, J = 7.4, 1.3 Hz). In THF-d_8, on the other hand, two sets of signals are detected (Figure 4). The minor one is found at δ (ppm) = 9.68 (s), 6.74 (d, J = 7.1 Hz), 6.42 (partly hidden), and 6.30 (partly hidden). The major component is observed at δ (ppm) = 8.55 (s), 6.56 (dd, J = 7.7, 1.5 Hz), 6.47 (t, J = 7.7 Hz), and 6.33 (dd, J = 7.7, 1.5 Hz). The signal of the aldehyde proton of **4** serves as a spectroscopic probe and allows us to distinguish between the mono- and dinuclear complexes. In the monomer, the resonance appears at δ (ppm) = 9.68, a typical shift for aromatic aldehydes. In the dimer, on the other hand, a highfield shift of more than 1 ppm to δ (ppm) = 8.55 occurs. The crystal structure of the dimer provides an idea why this upfield shift is observed. The aldehyde proton of each of the six ligands is located in close proximity to the center of the aromatic system of another ligand at the second complex unit. Consequently, the aldehyde protons in the dimer experience a strong anisotropic deshielding effect which is absent in the monomer.

^{7}Li NMR spectroscopy is a tool to distinguish between lithium cations which are bound in the dimer and those which are solvated.[28] In DMSO-d_6, only the monomer $[(\mathbf{4})_3Ti]^{2-}$ is present. Therefore only one signal of solvated ions is observed by ^{7}Li NMR at $\delta = -0.53$ ppm. In THF-d_8, signals are observed at δ = 0.41 ppm for solvated Li^+ and at δ = 1.82 ppm for Li^+ bound in the dimer (Figure 5). For the gallium(III) complex "$Li_3[(\mathbf{4})_3Ga]$" similar NMR spectroscopic results are obtained. The fact that two distinct sets of signals are observed for monomer and dimer in all cases provides evidence for an equilibration between

(27) For a related solvent effect of DMSO in the coordination of templating cations, see: Albrecht, M.; Janser, I.; Runsink, J.; Raabe, G.; Weis, P.; Fröhlich, R. *Angew. Chem.* **2004**, *116*, 6832−6836; *Angew. Chem., Int. Ed.* **2004**, *43*, 6662−6666.
(28) Albrecht, M. *Chem.−Eur. J.* **1997**, *3*, 1466−1471.

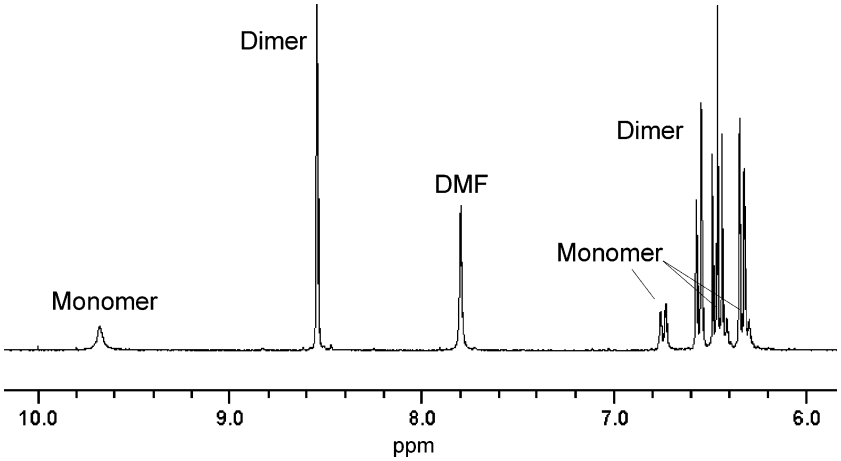

Figure 4. ^{1}H NMR spectrum of "$Li_2[(\mathbf{4})_3Ti]$" in THF-d_8 showing two sets of signals corresponding to both the monomer and the dimer.

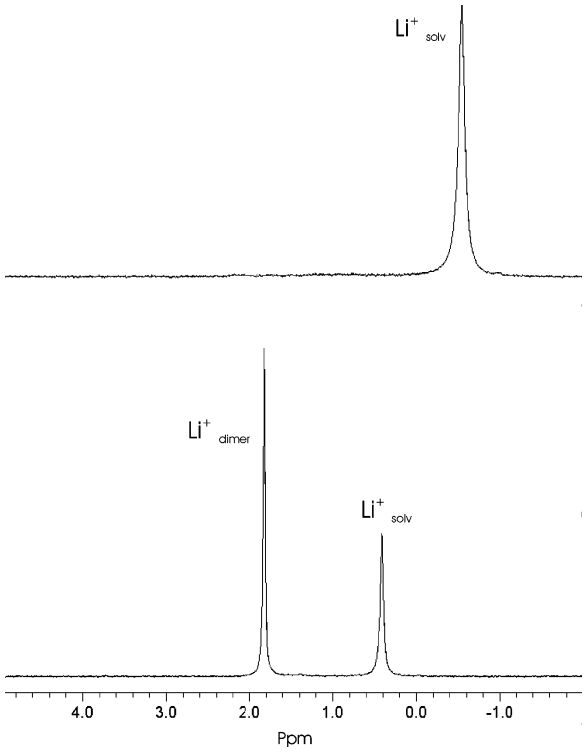

Figure 5. ^{7}Li NMR spectra of "$Li_2[(\mathbf{4})_3Ti]$" in DMSO-d_6 (top) showing the signal of solvated lithium cations and in THF-d_8 (bottom) showing an additional signal for Li^+ bound in the dimer.

both which is slow on the NMR time scale of the ^{1}H as well as the ^{7}Li NMR experiment.

To unambiguously ascertain the assignment of the resonances of dimer and monomer of $Li_2[(\mathbf{4})_3Ti]$ and $Li_3[(\mathbf{4})_3Ga]$, we performed DOSY NMR measurements.[29] For the titanium complexes in acetone-d_6 at 298 K, we obtained diffusion coefficients of $D = 8.94\ 10^{-10}$ m^2/s (monomer) and of $D = 7.89\ 10^{-10}$ m^2/s (dimer). Assuming an approximate spherical shape for the monomer as well as the dimer, we can calculate a ratio of the volumes of monomer/dimer = 1:1.27. In case of the gallium analogues (Figure 6), the measurements (DMSO-d_6, 298 K) lead to $D = 1.85\ 10^{-10}$ m^2/s for the monomer and $D = 1.45\ 10^{-10}$ m^2/s for the dimer with a calculated ratio of "spherical" volumes of monomer/dimer 1:2.04. These differences in the mobility and the calculated "size ratios" between the titanium(IV) and gallium(III) complexes are possibly due to differences in solvation in the highly polar DMSO-d_6 versus the relatively unpolar acetone-d_6 and different charges of the compounds.

From the integral ratios of monomer and dimer signals in the ^{1}H NMR spectra, the dimerization constants K_{dim} and the changes of free enthalpies ΔG_{dim} easily can be calculated (Table 1). We find the stabilization of the dimer to strongly depend on the donating ability of the solvent. For example, only the monomer is observed for $Li_2[(\mathbf{4})_3Ti]$ in DMSO-d_6 at 298 K. DMSO is a good ligand for lithium and therefore is a strong competitor for dimer formation. Lowering the donor ability of the solvent by use of methanol-d_4, THF-d_8, or even acetone-d_6 leads to high dimerization constants K_{dim}. Related solvent effects are observed for the gallium(III) complex. However, here the dimer is more stable than it was observed for the corresponding titanium(IV) complexes. Probably, the higher charge of the trianion $[(\mathbf{4})_3Ga]^{3-}$ as compared to the dianion $[(\mathbf{4})_3Ti]^{2-}$ leads to a tighter "electrostatic" binding of the lithium cations and to a higher stability of the dimer.

The influence of the solvent on the dimer−monomer equilibrium of $Li_2[(\mathbf{4})_3Ti]$ and $Li_3[(\mathbf{4})_3Ga]$ allows tuning the ratio between the two species over a wide range. Figure 7 shows the percentage of titanium(IV) ions which are bound in the monomeric $Li_2[(\mathbf{4})_3Ti]$ or dimeric $Li_4[(\mathbf{4})_6Ti_2]$, respectively, depending on the molar fraction of the solvent mixture THF-d_8/methanol-d_4.

Temperature-dependent ^{1}H NMR measurements of the dimerization equilibria of $Li_2[(\mathbf{4})_3Ti]$ (THF-d_8, $concn_{Ti} = 8.0$ mM) and $Li_3[(\mathbf{4})_3Ga]$ (DMSO-d_6, $concn_{Ga} = 8.0$ mM) permit extraction of thermodynamic data (see Figure 8). The data show the dimerization of the monomers in both examples to be enthalpically (Ti: $\Delta H_{dim} = -12.6(4)$ kJ/mol. Ga: $\Delta H_{dim} = -9.1(2)$ kJ/mol) as well as entropically (Ti: $\Delta S_{dim} = +16(1)$ J/mol. Ga: $\Delta S_{dim} = +4(1)$ J/mol) favored. The latter is probably due to the liberation of solvent molecules upon binding of lithium cations in the dimers $[Li_3(\mathbf{4})_6Ti]^-$ and $[Li_3(\mathbf{4})_6Ga_2]^{3-}$, respectively.[30]

(29) (a) Cohen, Y.; Avram, L.; Frish, L. *Angew. Chem.* **2005**, *116*, 524−560; *Angew. Chem., Int. Ed.* **2005**, *44*, 520−554. (b) Johnson, C. S., Jr. *Prog. Nucl. Magn. Reson. Spectrosc.* **1999**, *34*, 203−256.

(30) (a) Mamula, O.; Monlien, F. J.; Porquet, A.; Hopfgartner, G.; Merbach, A. E.; von Zelewsky, A. *Chem.−Eur. J.* **2001**, *7*, 533−539. (b) Bark, T.; Duggeli, M.; Stoeckli-Evans, H.; von Zelewsky, A. *Angew. Chem.* **2001**, *113*, 2924−2927; *Angew. Chem., Int. Ed.* **2001**, *40*, 2848−2851.

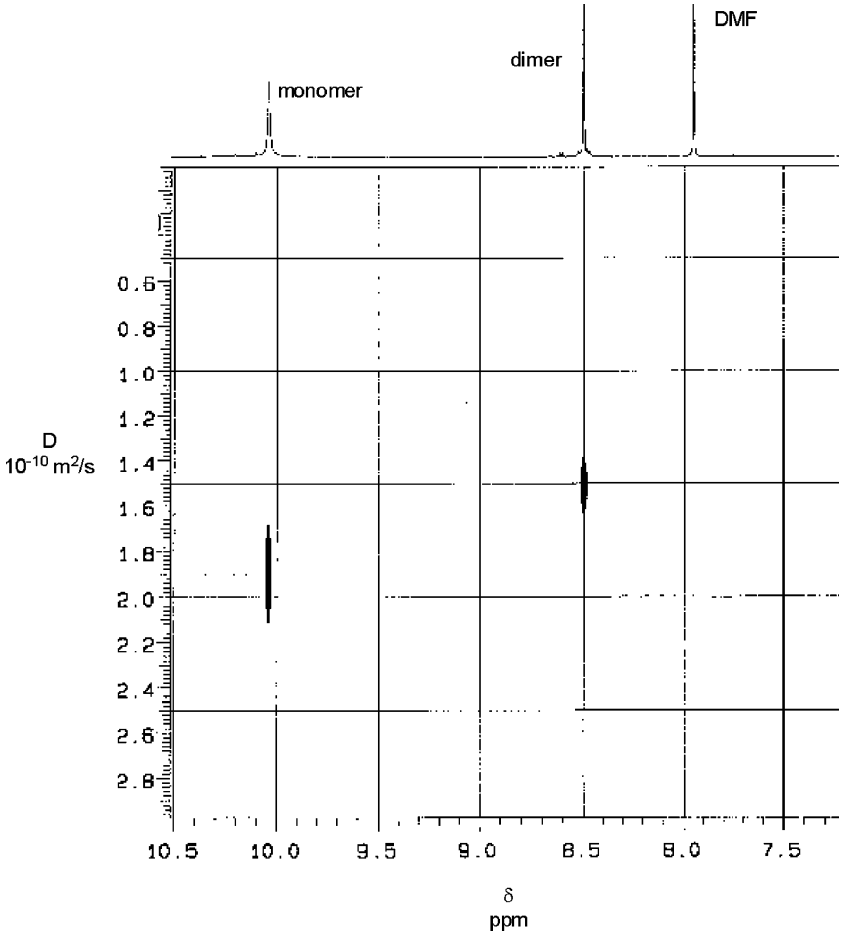

Figure 6. Part of the DOSY NMR spectrum (DMSO-d_6, 298 K) of $Li_3[(\mathbf{4})_3Ga]$ and $Li_6[(\mathbf{4})_6Ga_2]$.

Table 1. Dimerization Constants K_{dim} = [Dimer]/[Monomer]^2 and ΔG_{dim} Values Observed for the Monomer−Dimer Equillibria in Different Solvents at 298 K

	$2Li_2[(\mathbf{4})_3Ti] \rightleftharpoons L4[(\mathbf{4})_6Ti_2]$		$2Li_3[(\mathbf{4})_3Ga] \rightleftharpoons Li_6[(\mathbf{4})_6Ga_2]$	
solvent	K_{dim} [M^{-1}]	ΔG_{dim} [kJ/mol]	K_{dim} [M^{-1}]	ΔG_{dim} [kJ/mol]
DMSO-d_6	only monomer		80	−10.86
D_2O	only monomer		1600	−18.28
CD_3OD	10	−5.70	200.000	−30.24
THF-d_8	950	−16.99	low solubility	
acetone-d_6	1330	−17.82	low solubility	

As described for the complexes of the aldehyde-substituted ligand **4**, dimer−monomer equilibria can be also observed for the complexes of the ketones **5a**−**j**, **6a,b**, and of the esters **7a,b** in solution. Figure 9 shows the ^{1}H NMR signals of the *n*-propyl groups of $Li_2[(\mathbf{5c})_3Ti]$ and $Li_4[(\mathbf{5c})_6Ti_2]$ in methanol-d_4. The resonances of the monomeric species are observed at $\delta = 3.06$ (t, $J = 7.4$ Hz, CH_2), 1.59 (sextet, $J = 7.4$ Hz, CH_2), and 0.85 (t, $J = 7.4$ Hz, CH_3), while the dimer is observed as the major species at $\delta = 2.68$, 1.96 (2 m, CH_2), 1.10, 0.98 (2 m, CH_2), and 0.63 (t, $J = 7.7$ Hz, CH_3). As described for the aldehyde protons of **4**, the anisotropic high-field shift of the *n*-propyl group in $Li_4[(\mathbf{5c})_6Ti_2]$ is due to its location above the center of the aromatic ring of another ligand **5c**.

A major difference between monomer $Li_2[(\mathbf{5c})_3Ti]$ and dimer $Li_4[(\mathbf{5c})_6Ti_2]$ is the diastereotopic splitting of the CH_2 resonances observed for the CH_2 groups of the dimer.[31] In the monomer, only an averaged set of signals is observed which is due to a fast inversion of configuration at the metal center. The binding of lithium cations in the dimer slows down the racemization. Diastereotopicity is thus observed, because this process is slow on the NMR time scale. Similar spectroscopic behavior is observed for the complexes of ligands **5b**−**j** and **7b**. The

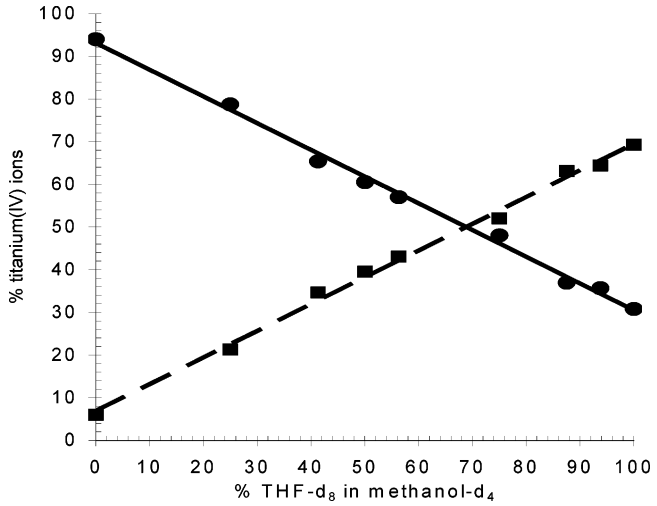

Figure 7. Percentage of titanium(IV) ions bound in the monomer (●) and dimer (■) depending on the composition of a solvent mixture of THF-d_8 and methanol-d_4 (concn$_{Ti}$ = 7.5 mmol/L).

(31) (a) Kersting, B.; Meyer, M.; Powers, R. E.; Raymond, K. N. *J. Am. Chem. Soc.* **1996**, *118*, 7221−7222. (b) Albrecht, M.; Schneider, M.; Röttele, H. *Chem. Ber./Recueil* **1997**, *130*, 615−619.

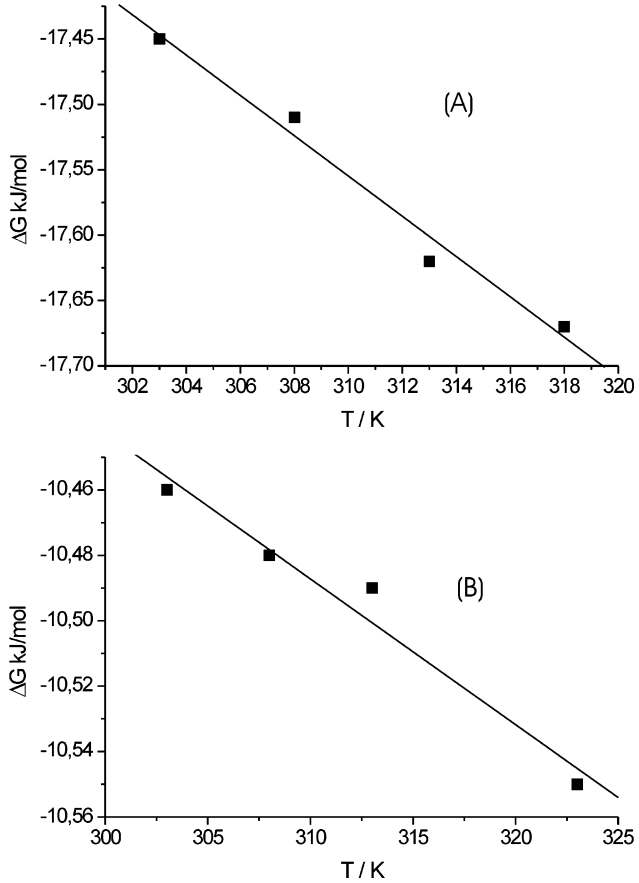

Figure 8. Plot of $\Delta G_{dim}(T)$ (kJ/mol) versus temperature (K) for the dimerization of $Li_2[(\mathbf{4})_3Ti]$ (A) (THF-d_8, $concn_{Ti} = 8.0$ mmol/L) and $Li_3[(\mathbf{4})_3Ga]$ (B) (DMSO-d_6, $concn_{Ga} = 8.0$ mmol/L).

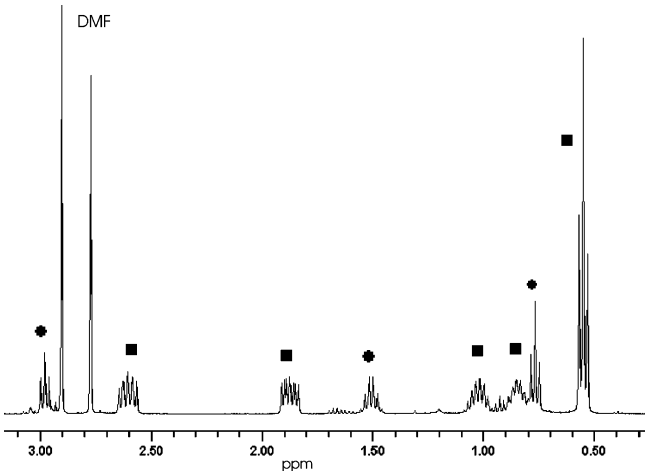

Figure 9. Part of the NMR spectrum of $Li_2[(\mathbf{5c})_3Ti]$ (●) and $Li_4[(\mathbf{5c})_6Ti_2]$ (■) in methanol-d_4 showing the signals of the *n*-propyl substituent.

surprisingly high barrier for the dimer/monomer equilibrium should be due to the simultaneous (and probably cooperative) formation of twelve lithium−oxygen bonds.

Due to the slow exchange between monomer and dimer, ^{1}H NMR measurements of $Li_2[(\mathbf{L})_3Ti]$ (L = **5a**−**j**-H_2, **6a**-H_2, **7a,b**-H_2) in methanol-d_4 at 298 K easily yield the dimerization constants K_{dim} and the free dimerization enthalpies ΔG_{dim} (Table 2) and permit a comparison of different substituents at the carbonyl group. Dimer formation correlates with the donor strength of the type of carbonyl unit at the ligand. Aldehydes

Table 2. Dimerization Constants K_{dim} = [Dimer]/[Monomer]^2 and ΔG_{dim} Values Observed for the Monomer−Dimer Equillibria of the Titanium Complexes $Li_2[(L)_3Ti]$ in Methanol-d_4 at 298 K

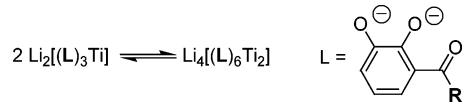

ligand L	R	K_{dim} [M^{-1}]	ΔG_{dim} [kJ/mol]	ligand L	R	K_{dim} [M^{-1}]	ΔG_{dim} [kJ/mol]
4	H	10	−5.7	**5g**	*n*-C_7H_{15}	725	−16.3
5a	CH_3	3715	−20.4	**5h**	*n*-C_8H_{17}	1425	−18.0
5b	C_2H_5	785	−16.5	**5i**	*n*-$C_{10}H_{19}$	665	−16.1
5c	*n*-C_3H_7	1110	−17.4	**5j**	*n*-$C_{12}H_{25}$	1200	−17.6
5d	*n*-C_4H_9	1500	−18.1	**6a**	*i*-C_3H_7	3.6	−3.2
5e	*n*-C_5H_{11}	1015	−17.2	**7a**	OCH_3	25 600	−25.2
5f	*n*-C_6H_{13}	965	−17.0	**7b**	OC_2H_5	only dimer	

such as **4** are the weakest donors, leading to the lowest K_{dim} = 10 M^{-1}, while the strongly donating ester groups as in **7** favor formation of the dimer (K_{dim} = 25 600 M^{-1}). The ketones **5a**−**j** are donors of intermediate strengths and thus lead to intermediate K_{dim} = 665−3715 M^{-1}.

For the complexes of the ketones **5a**−**j** and **6a**, we furthermore observe a steric effect on the dimerization equilibrium. $Li_2[(\mathbf{5a})_3Ti]$, with its small methyl side chain, shows a high tendency for dimerization (K_{dim} = 3715 M^{-1}). Steric bulk in the longer *n*-alkyl substituted complexes $Li_2[(\mathbf{5b}-\mathbf{j})_3Ti]$ results in a lower K_{dim} = 665−1500 M^{-1}, while for $Li_2[(\mathbf{6a})_3Ti]$ with the branched isopropyl substituent dimerization is highly unfavored (K_{dim} = 3.6 M^{-1}). Within the series of *n*-alkyl substituted complexes $Li_2[(\mathbf{5b}-\mathbf{j})_3Ti]$, quite similar free enthalpies of dimerization are determined and a large effect of the chain length is not observed. The trend to higher dimerization constants for the Ga complexes discussed above for the aldehyde ligand **4** is also observed for ketone **5a**: "$Li_3[(\mathbf{5a})_3Ga]$" shows a dimerization constant in DMSO-d_6 at 298 K of K_{dim} = 5200 M^{-1}, while the corresponding Ti complex $Li_2[(\mathbf{5a})_3Ti]$ hardly forms dimers under the same conditions (K_{dim} = 10 M^{-1}).

Our solution phase NMR spectroscopic studies clearly show the equilibrium between monomer and dimer to depend on different factors. Dimerization is only observed when the cation mediating it has the appropriate size. For Na^+ and K^+, no dimer formation is found, while Li^+ efficiently mediates the formation of dinuclear helicate-like complexes. Dimer formation is also favored when the bridging lithium cations are strongly bound. This is the case (i) if the mononuclear complex units bear a high negative charge (e.g., $Li_6[(\mathbf{4})_6Ga_2]$ versus $Li_4[(\mathbf{4})_6Ti_2]$), (ii) if solvents with a low tendency to solvate lithium are present (e.g., acetone versus DMSO), (iii) if the carbonyl oxygen is a strong donor (e.g., ester versus aldehyde), and (iv) if the steric bulk at the carbonyl oxygen is low (e.g., methyl ketone versus the corresponding isopropyl analogue). Some of these effects cancel each other to some extent. For example, aldehyde ligand **4** has a lower donor strength disfavoring dimerization as compared to ketones **5a**−**j** but also a low steric demand favoring it. The detailed analysis of these effects permits control of the dimerization equilibrium quite precisely over a wide range.

Solution Studies: ESI Mass Spectrometry. Negative ion electrospray ionization Fourier transform ion-cyclotron-resonance (ESI FT-ICR) mass spectrometry shows the presence of dimeric as well as monomeric complexes in solution.[32] The compounds were either sprayed from THF or THF/methanol

(1:1). With titanium(IV) as metal center, signals for monoanions $[Li_3(\mathbf{4}-\mathbf{7})_6Ti_2]^-$ and $[Li(\mathbf{4}-\mathbf{7})_3Ti]^-$ are observed in quite clean mass spectra. In addition, sometimes low-intensity signals are observed for monomers $[H(\mathbf{4}-\mathbf{7})_3Ti]^-$ that underwent the exchange of the Li^+ cation against a proton. The intensities reflect semiquantitatively the concentrations in solution as determined by NMR spectroscopy. However, since the ESI response factors[33] are not known, we refrain from drawing quantitative conclusions. For the gallium(III) compounds, the mass spectra are more complex. Monomeric $[LiH(\mathbf{4})_3Ga]^-$ (m/z = 485) and $[LiH(\mathbf{5a})_3Ga]^-$ (m/z = 527), respectively, are detected in addition to dimeric species in several charge states: $[Li_4(\mathbf{4})_6Ga_2]^{2-}$ (m/z = 491), $[Li_3(\mathbf{4})_6Ga_2]^{3-}$ (m/z = 326), $[Li_4(\mathbf{5a})_6Ga_2]^{2-}$ (m/z = 534), and $[HLi_4(\mathbf{5b})_6Ga_2]^-$ (m/z = 1069). In addition, monomeric species with only two ligands $[(\mathbf{4})_2Ga]^-$ (m/z = 341) and $[(\mathbf{5a})_2Ga]^-$ (m/z = 369) were detected as fragments (vide infra).

As shown below, the spectra obtained under soft electrospray ionization conditions reflect the species present in solution. Harsher ionization conditions significantly increase the abundances of mononuclear ions at the expense of the dimeric complexes due to fragmentation during the ionization process. Consequently, some caution is required to get a true picture of the species present in solution.

Beyond analytical characterization, mass spectrometry is a valuable tool for following solution phase processes kinetically when they meet the time scale of the experiment.[34] When the crystalline dimeric complexes are dissolved in a 1:1 mixture of THF and methanol as the spray solvent, the relatively slow dissociation of the dimers into the corresponding monomers can be followed easily (Figure 10). Since the crystalline material contains only dimers (see above), initially, dimeric ions are observed almost exclusively. During 2 days at room temperature, the dimers almost completely dissociate into the corresponding monomers, seemingly a contradiction to the NMR experiments in which significant amounts of dimers were observed in equilibrium with the monomers for this solvent mixture (for example, see Figure 7). However, one needs to take into account that the concentration of the solution used in the MS experiments is lower than that used for NMR analysis by a factor of about 50. In view of the low binding constants ($Li_2[(\mathbf{5f})_3Ti]$: K_{dim} (methanol) = 965 M^{-1}), the complete dissociation of the dimer thus does not come as a surprise.

In a second experiment, we intended to study the formation of heterodinuclear complexes from a mixture of two different homodimers. Two 0.4 mM solutions of the titanium(IV) complexes $Li_2[(\mathbf{5f})_3Ti]$ and $Li_2[(\mathbf{5g})_3Ti]$ were mixed in THF/MeOH = 1:1 and the exchange behavior was followed over time by ESI FT-ICR mass spectrometry (Figure 11a). For comparison, the same experiment was performed in pure THF as the spray solvent (Figure 11b). Due to the similar lengths of the alkyl chains, similar properties, in particular similar ESI response factors, are expected for both types of complexes.

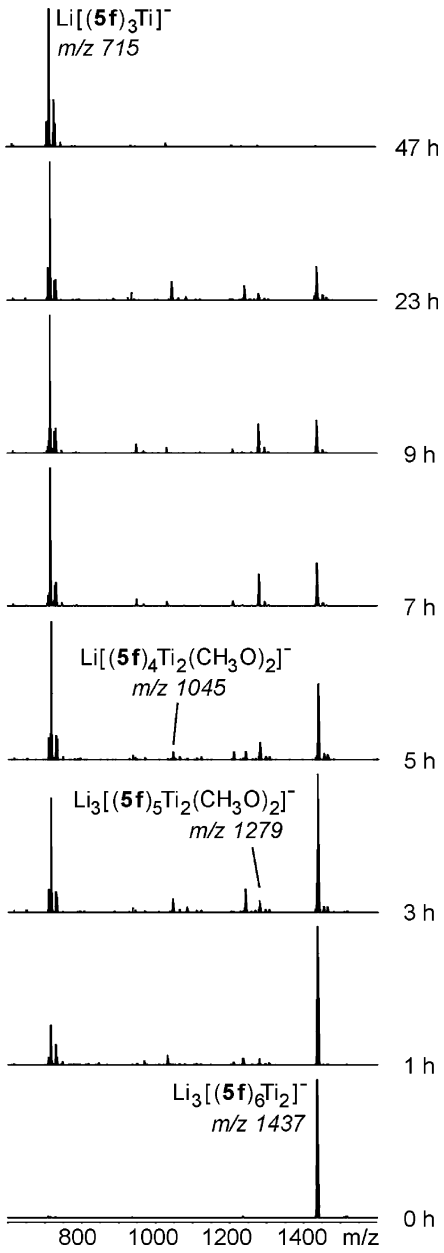

Figure 10. Negative ESI FTICR mass spectra of a 100 μM solution of dimeric $Li_4[(\mathbf{5f})_6Ti_2]$ in THF/MeOH = 1:1 after different time intervals. Note that the concentrations used in the MS experiment are far below those of the NMR experiments. Consequently, the dimer finally dissociates completely into the two monomers.

The ESI mass spectra recorded directly after mixing the two solutions exhibit signals for the heterodinuclear complexes hardly above the signal-to-noise ratio (Figure 11, bottom traces). This provides evidence for a quite slow exchange of monomers within the dimer irrespective of the solvent mixture. Interestingly, the monomer ions observed in the spectrum obtained from the THF/MeOH mixture reveal complete exchange of the catechol ligands. A roughly 1:3:3:1 statistical ratio is observed for the A_3, A_2B, AB_2, and B_3 complexes (inset in Figure 11a, bottom trace; A = **5f**, B = **5g**). The fact that the ligand exchange

(32) For recent MS studies on metallosupramolecular aggregates, see: (a) Marquis-Rigault, A.; Dupont-Gervais, A.; Baxter, P. N. W.; Van Dorsselaer, A.; Lehn, J.-M. *Inorg. Chem.* **1996**, *35*, 2307−2310. (b) König, S.; Brückner, C.; Raymond, K. N.; Leary, J. A. *J. Am. Soc. Mass Spectrom.* **1998**, *9*, 1099−1103. (c) Hopfgartner, G.; Vilbois, F.; Piguet C. *Rap. Commun. Mass Spectrom.* **1999**, *13* 302−306. (d) Sakamoto, S.; Fujita, M.; Kim, K.; Yamaguchi, K. *Tetrahedron* **2000**, *56*, 955−964. (e) Ziegler, M.; Miranda, J. J.; Andersen, U. N.; Johnson, D. W.; Leary, J. A.; Raymond, K. N. *Angew. Chem.* **2001**, *113*, 755−758; *Angew. Chem., Int Ed.* **2001**, *40*, 733−736. (f) Schalley, C. A.; Müller, T.; Linnartz, P.; Witt, M.; Schäfer, M.; Lützen, A. *Chem.—Eur. J.* **2002**, *8*, 3538−3551. (g) Müller, I. M.; Möller, D.; Schalley, C. A. *Angew. Chem.* **2005**, *117*, 485−488; *Angew. Chem., Int. Ed.* **2005**, *44*, 480−484.

(33) Leize, E.; Jaffrezic, A.; Van Dorsselaer, A. *J. Mass Spectrom.* **1996**, *31*, 537−544.

(34) (a) Romero, F. M.; Ziessel, R.; Dupont-Gervais, A.; Van Dorsselaer, A. *Chem. Commun.* **1996**, 551−552. (b) Marquis-Rigault, A.; Dupont-Gervais, A.; Van Dorsselaer, A.; Lehn, J.-M. *Chem.—Eur. J.* **1996**, *2*, 1395−1398.

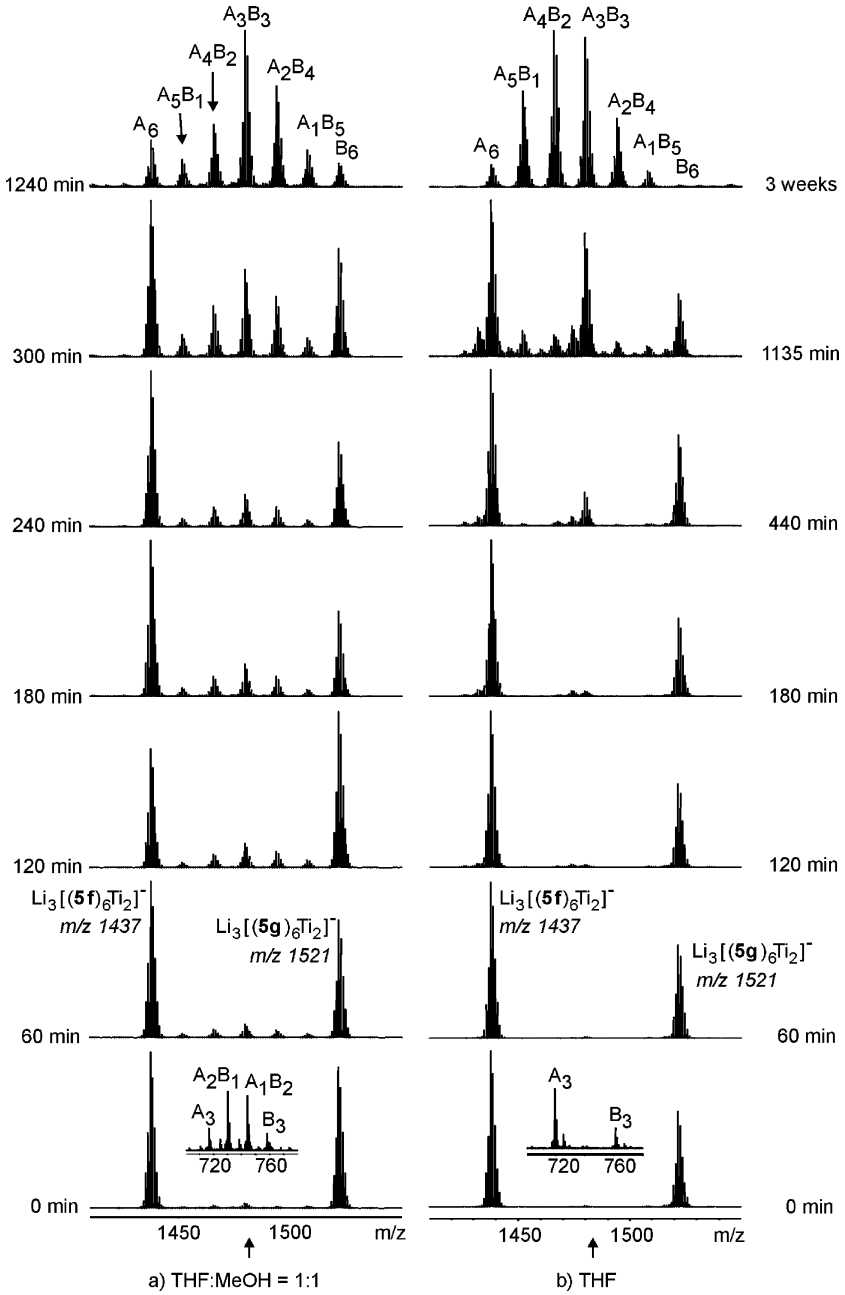

Figure 11. Stack plots of the ESI FT-ICR spectra of a 1:1 mixture of $Li_2[(\mathbf{5f})_3Ti]$ and $Li_2[(\mathbf{5g})_3Ti]$ (a) in THF/methanol 1:1 and (b) in pure THF after different time intervals at room temperature. The insets in the bottom spectra show the monomer region directly after mixing. While the catecholates of the monomeric complexes are quickly exchanged in THF/MeOH, they exchange much more slowly in pure THF.

is fast for the monomeric complexes under study, while the dimers appear only as homodinuclear complexes, confirms that the mass spectra reflect the situation in solution. If the ionization conditions were too harsh and the monomers were formed during the ionization process, one would expect to see much more intense signals for A_3 and B_3 complexes. If in turn the dimers were formed from the monomers by what is often called "unspecific aggregation" during the electrospray ionization, one would expect to see a statistical mixture of all possible species. Both are not the case, and we can thus safely conclude that the monomers and dimers examined are already present in solution.

In pure THF, the A_2B and AB_2 monomers are hardly visible. Consequently, the exchange of catecholate ligands is slow here. This can easily be rationalized by invoking methanol as a solvent which accelerates the catecholate exchange due to its protic nature. In the absence of methanol, this exchange then slows down significantly. In THF alone, the expected heterodinuclear complexes are indeed formed. Initially, the signals for dimers $Li_3[(\mathbf{5f})_6Ti_2]^-$ (m/z = 1437) and $Li_3[(\mathbf{5g})_6Ti_2]^-$ (m/z = 1521) are observed as the dominating species. Only a minor trace of mixed dimer $Li_3[(\mathbf{5f})_3(\mathbf{5g})_3Ti_2]^-$ (m/z = 1480) is found. Over time, this signal increases and the spectrum recorded 1135 min after mixing shows three prominent signals for the two homo- and the heterodinuclear complexes. Such a result is in agreement with the assumption that the exchange of individual catecholate ligands is slower than the exchange of complete monomeric complexes for both the dimeric and the monomeric complexes. The two monomer units incorporated in the dimer are thus homoleptic. Catecholate exchange nevertheless occurs to some extent, and the spectrum obtained after 3 weeks corresponds to

an almost statistical mixture of all possible dimeric species, i.e., A_6, A_5B, A_4B_2, A_3B_3, A_2B_4, AB_5, and B_6 complexes (A = **5f**, B = **5g**).

The same experiment performed in THF/MeOH = 1:1 clearly leads to a different result. Initially, the two homodinuclear complexes are most prominent. Over time, however, not only the expected heterodinuclear A_3B_3 ion $Li_3[(\mathbf{5f})_3(\mathbf{5g})_3Ti_2]^-$ (m/z = 1480) is observed but also a statistical mixture of all possible dimers grows between the two homodimer signals. This behavior is only in agreement with dimers dissociating into monomers, which undergo a fast catecholate exchange and then reassociate to some extent to yield all possible mixed dimers. In contrast, ligand exchange within the dimer is not observed due to the additional binding energy provided by the coordination to the bridging lithium cations. In this case, one would expect to initially observe a "U-shaped" distribution of the different exchange products which more and more develops toward the statistical distribution.

Consequently, mass spectrometry is a valuable tool for gathering qualitative mechanistic insight into the exchange equilibria in solution. Since the two dimers initially differed only by an additional methylene group, an NMR spectroscopic analysis of the same processes is hampered by signal overlap and both methods yield complementary data.

Gas-Phase Reactivity of the Dimeric Complexes. Mass spectrometry not only permits us to examine the solution-phase reactivity of the complexes under study but also allows us to study their reactivity in the gas phase by tandem MS experiments. The collision-induced decay (CID) of mass-selected homodinuclear $[Li_3(\mathbf{4})_6Ti_2]^-$ (m/z = 933; Figure 12c), $[Li_4(\mathbf{4})_6Ga_2]^{2-}$ (m/z = 491), $[Li_3(\mathbf{4})_6Ga_2]^{3-}$ (m/z = 326; Figure 12d), and $[Li_3(\mathbf{5-7})_6Ti_2]^-$ was studied in the gas phase by MS/MS experiments with argon as the collision gas.[35] The three stages of this experiment are shown in Figure 12. Trace a shows a typical mass spectrum of $[Li_4(\mathbf{4})_6Ti_2]$ which contains intense signals for dimer $[Li_3(\mathbf{4})_6Ti_2]^-$. This ion is then mass selected (trace b) and subsequently collided with Ar gas. It fragments (trace c) into monomeric triscatecholate complexes ($[Li(\mathbf{4})_3Ti]^-$, m/z = 463). All titanium(IV) complexes $Li_2[(\mathbf{5-7})_3Ti]$ show the same reactivity in CID experiments. In a quasi-symmetrical reaction, the dimers $[Li_3(\mathbf{5-7})_6Ti_2]^-$ decompose into two monomeric units, one of which carries the negative charge ($[Li(\mathbf{5-7})_3Ti]^-$), while the other is neutral due to the presence of an additional Li^+ cation ($[Li_2(\mathbf{5-7})_3Ti]$).

Interestingly, the doubly and triply charged gallium complexes $[Li_4(\mathbf{4})_6Ga_2]^{2-}$ and $[Li_3(\mathbf{4})_6Ga_2]^{3-}$ were more labile and even at rather low collision energies decomposed in an asymmetric fashion quite similarly to each other but significantly different from the Ti analogues. $[Li_4(\mathbf{4})_6Ga_2]^{2-}$ fragmented into $[Li_4(\mathbf{4})_4Ga]^-$ (m/z = 635) and $[(\mathbf{4})_2Ga]^-$ (m/z = 341) and distributed the two charges over both fragments in order to reduce charge repulsion (Scheme 3). $[Li_3(\mathbf{4})_6Ga_2]^{3-}$ gave similar fragments: $[Li_3(\mathbf{4})_4Ga]^{2-}$ (m/z = 317) and $[(\mathbf{4})_2Ga]^-$ (m/z = 341) are formed. The lability of $[Li_3(\mathbf{4})_6Ga_2]^{3-}$ is due to the higher negative charge of the ion, which destabilizes the supramolecular aggregate and leads to a fast decomposition. This behavior is in contrast to the higher solution stability of the Ga complex as compared to their Ti analogues. However, in solution, solvent molecules and, in particular, counterions are present which contribute to compensating the higher negative charge and provide additional binding energy through electrostatic interactions with the counterions. In the gas phase, these counterions are absent, and thus charge repulsion destabilizes the multiply charged complexes.

To test, how a heterodinuclear complex $Li_5[(\mathbf{4})_6GaTi]$ would behave in view of these quite different fragmentation pathways, we prepared a 1:1 mixture of the two homodimers in THF and equilibrated it until a roughly statistical mixture of $Li_6[(\mathbf{4})_6Ga_2]$, $Li_4[(\mathbf{4})_6Ti_2]$, and $Li_5[(\mathbf{4})_6GaTi]$ was formed. Then, the ions

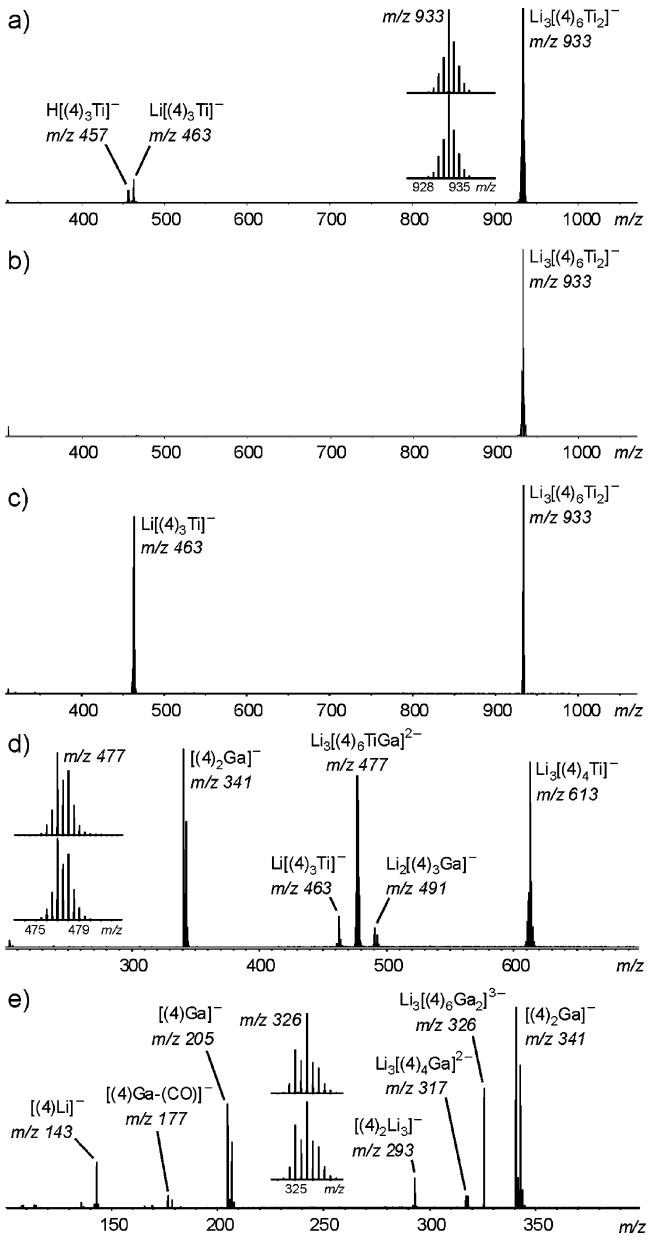

Figure 12. Spectra a−c correspond to the different stages of a tandem MS experiment: (a) Negative ion ESI FT-ICR mass spectrum of $Li_4[(\mathbf{4})_6Ti_2]$ sprayed from THF. (b) Same spectrum after mass selection of the dimer $[Li_3(\mathbf{4})_3Ti]^-$ (all isotopologues isolated). (c) Collision-induced decay (CID) mass spectrum of mass-selected $[Li_3(\mathbf{4})_3Ti]^-$ with Ar as the collision gas. (d) CID spectrum of mass-selected ions corresponding to the triply charged dimer $[Li_3(\mathbf{4})_6Ga_2]^{3-}$. (e) CID spectrum of mass-selected ions corresponding to the doubly charged heterodimer $[Li_3(\mathbf{4})_6GaTi]^{2-}$. Insets compare the experimental isotope patterns of the parent ions (top) with those calculated on the basis of natural abundances (bottom).

(35) (a) Schalley, C. A. *Int. J. Mass Spectrom.* **2000**, *194*, 11−39. (b) Schalley, C. A. *Mass Spectrom. Rev.* **2001**, *20*, 253−309.

Scheme 3. Gas-Phase Fragmentation Pathways[a]

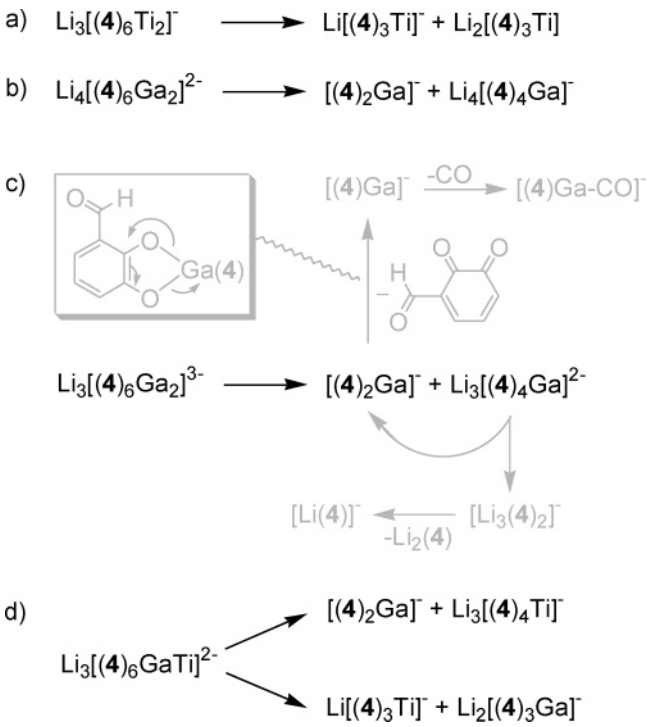

[a] (a) The singly charged homodinuclear titanium(IV) and (b) doubly and (c) triply charged gallium(III) complexes. (d) Fragmentation pathways of doubly charged heterodinuclear titanium(IV)/gallium(III) complexes of ligand **4**. With the number of charges, the complexity of the fragmentation reactions increases due to charge repulsion. The sequences in gray show consecutive decompositions of primarily formed species with the inset giving a probable fragmentation mechanism for the loss of one catecholate ligand from the $[(\mathbf{4})_2Ga]^-$ anion.

corresponding to the doubly charged heterodimer $[Li_3(\mathbf{4})_6GaTi]^{2-}$ at $m/z = 477$ were mass selected and subjected to collision-induced dissociation. This species decomposes following both pathways found for the two homodimers.[36] The asymmetric cleavage into $[(\mathbf{4})_2Ga]^-$ ($m/z = 340.96$) and $[Li_4(\mathbf{4})_4Ti]^-$ ($m/z = 613$) competes with dissociation into the two monomers $[Li(\mathbf{4})_3Ti]^-$ ($m/z = 463$) and $[Li_2(\mathbf{4})_3Ga]^-$ ($m/z = 491$) (Figure 12e). Both monomers appear as singly charged species minimizing charge repulsion. The observation of only one of the two possible asymmetric cleavages is probably due to the thermodynamically favored formation of $[(\mathbf{4})_2Ga]^-$ as a stable species which possesses a completely filled electron shell. The complexity of the fragmentation patterns and the extent of consecutive fragmentation reactions increase with the number of charges present in the complexes. Also, the charge distribution within the monomeric units appears to control the fragmentation pathways.

The gas phase experiments reveal a quite interesting difference in the reactivity of the titanium and gallium complexes. Significant differences in the stabilities of multiply charged ions in the gas phase and in solution can be traced back to the absence of the appropriate number of counterions in the gas phase. These results underline again the importance of the environment of a species under study. Properties observed in solution are always properties of the molecules within their environment. The intrinsic properties can be evaluated in the gas phase and may differ significantly.

(36) For a heterodimeric gallium/titanium helicate, see: Albrecht, M.; Fröhlich, R. *J. Am. Chem. Soc.* **1997**, *119*, 1656−1661.

Conclusions

In this paper, we described the eleven-component self-assembly of helicate type complexes, which are formed from six catechol ligands bearing carbonyl groups in their 3-position, two titanium(IV) (or gallium(III)) ions and three lithium cations. The formation of the compounds represents a hierarchical self-assembly process with a strong interaction between the metals and the catecholates and a weaker binding of the lithium cations which leads to dimerization. The monomer−dimer equilibrium can be observed in solution by NMR spectroscopy, and it is found that the dimer is favored, if the monomer bears a high negative charge, if the carbonyl units are good donor atoms for binding the bridging Li cations, if the solvent poorly solvates these cations and thus does not efficiently compete, and if the sterical hindrance exerted by the side chains attached to the carbonyl groups is minimized. ESI FT-ICR MS investigations show that the ligands are tightly bound in the dimer, so that ligand scrambling only occurs in the monomeric species. This is in excellent agreement with the finding that diastereotopic signals for the methylene groups in the side chains of the ketone complexes are only seen in the NMR spectra for the dinuclear complexes. Complexation to the bridging lithium cations thus also suppresses the inversion of chirality. In the gas phase, the dinuclear titanium(IV) and gallium(III) complexes show different fragmentation pathways in CID experiments, with a symmetric cleavage in case of the titanium species and an unsymmetric decomposition of the gallium compounds. Data from the solid state, from solution, and from the gas phase contribute to a detailed understanding of the structural factors which govern thermodynamic as well as kinetic stabilities and the exchange mechanisms operative in solution.

The complexes presented in this contribution can be switched between their monomeric and dimeric forms by different factors. A precise control of these factors even permits us to fine-tune the monomer/dimer ratio. At present, we aim at substituting the side chains of these species to introduce specific functions which can be controlled by this switching process through control of the monomer−dimer equilibrium.

Experimental Section

General Remarks. NMR spectra were recorded on a Varian Mercury 300, Inova 400, or a Unity 500 spectrometer. FT-IR spectra were recorded by diffuse reflection (KBr) on a Bruker IFS spectrometer. Mass spectra (EI, 70 eV; FAB with 3-NBA as matrix) were measured on a Finnigan MAT 90, 95, or 212 mass spectrometer. FT-ICR ESI mass spectra were measured on a Bruker APEX IV FT mass spectrometer. Elemental analyses were obtained with a Heraeus CHN-O-Rapid analyzer. Melting points: Büchi B-540 (uncorrected). Chemicals were used as received by commercial suppliers. **4**-H_2 was purchased from Aldrich.

Negative ESI FT-ICR Mass Spectrometry. ESI mass spectra and MS/MS spectra were recorded on a Bruker APEX IV Fourier transform ion-cyclotron-resonance (FT-ICR) mass spectrometer with an Apollo electrospray ion source equipped with an off axis 70° spray needle. Typically, tetrahydrofuran (THF) or 1:1 mixtures of THF and methanol served as the spray solvents, and 100 μM solutions of the analytes were used. Analyte solutions were introduced into the ion source with a Cole-Parmers Instruments (Series 74900) syringe pump at flow rates of ca. 3−4 μL/min. Ion transfer into the first of three differential pump stages in the ion source occurred through a glass capillary with a 0.5 mm inner diameter and nickel coatings at both ends. Ionization parameters were adjusted as follows: capillary voltage, +4.5 kV;

endplate voltage, +4.0 kV; capexit voltage, −120 V; skimmer voltages, −20 to −10 V; temperature of drying gas, 250 °C. The flow of the drying gas was kept in a medium range, while the flow of the nebulizer gas was low. With the gas flows and the capexit voltage, the ratio of monomeric to dimeric ions can be changed over a wide range, since collisions with residual gas may lead to fragmentation of the dimer into the corresponding monomers. It is therefore crucial to set these parameters to as soft as possible conditions. The ions were accumulated in the instruments hexapole for 1.2 s. The ions are then introduced into the FT-ICR cell which was operated at pressures below 10^{-10} mbar and detected by a standard excitation and detection sequence. For each measurement 16 to 64 scans were averaged to improve the signal-to-noise ratio.

For the experiments aimed at following the kinetics of monomer and ligand exchange in solution, two of the sample solutions were mixed and mass spectra were recorded at different time intervals.

For MS/MS experiments, the whole isotope pattern of the ion of interest was isolated by applying correlated sweeps. Isolation of only the major isotope peak is possible, but in view of the particular isotope patterns of Ti and Ga complexes, the analysis of the fragmentation products is facilitated, when their isotope patterns are analyzed. Thus, for most of the tandem MS experiments described here, all isotopologues were subjected to the CID experiments. After isolation, argon was introduced into the ICR cell through a pulsed valve at a pressure of ca. 10^{-8} mbar, and the ions were accelerated by a standard excitation protocol. A sequence of several different spectra was recorded at different excitation pulse attenuations in order to get at least a rough and qualitative idea of the effects of different collision energies. Between excitation and detection, a 2 s pumping delay allowed the ions to react.

General Procedure for the Addition of Grignard Reagents to 2,3-Dimethoxybenzaldehyde.[21] A few drops of the bromide are added to the magnesium (0.01 mol) in a small amount of ether. After the reaction has started, the remaining bromide (in total 0.01 mol) is dissolved in ether (10 mL) and added. The mixture is refluxed until the magnesium is dissolved (approximately 30 min). The aldehyde is added, and the solution is heated for an additional 2 h. After cooling, the mixture is poured on ice, and concentrated HCl is added until the precipitate dissolves. The water is extracted with ether (2×), and the organic phase is washed with aqueous $NaHSO_3$, $NaHCO_3$, and a small amount of water. After drying with Na_2SO_4, solvent is removed in vacuo. The compounds are used without further purification. Therefore some of the alcohols are only characterized by NMR spectroscopy. However, if necessary, further purification can be done by column chromatography over silica gel.

1-(2,3-Dimethoxyphenyl)-1-ethanol.[37] Yield: 576 mg (quant) of crude product by addition of methyllithium instead of the Grignard reagent, yellow solid. ^{1}H NMR ($CDCl_3$, 400 MHz): δ (ppm) = 7.12 (t, J = 7.9 Hz, 1 H), 7.04 (dd, J = 7.9, 1.7 Hz, 1 H), 6.91 (dd, J = 7.9, 1.7 Hz, 1 H), 5.20 (q, J = 6.4 Hz, 1 H), 3.95 (s, 3 H), 3.92 (s, 3 H), 1.56 (d, J = 6.4 Hz, 3 H).

1-(2,3-Dimethoxyphenyl)-1-propanol.[21] Yield: 1.425 g (90%) of crude product, colorless liquid. ^{1}H NMR ($CDCl_3$, 400 MHz): δ (ppm) = 7.04 (t, J = 8.0 Hz, 1 H), 6.94 (dd, J = 8.0, 1.5 Hz, 1 H), 6.83 (dd, J = 8.0, 1.5 Hz, 1 H), 4.84 (dd, J = 7.4, 5.8 Hz, 1 H), 3.86 (2s, 3 H each), 1.80 (m, 2 H), 0.95 (t, J = 7.4 Hz, 3 H). ^{13}C NMR ($CDCl_3$, 100 MHz): δ (ppm) = 152.2 (C), 146.2 (C), 137.7 (C), 123.9 (CH), 118.6 (CH), 111.2 (CH), 71.4 (CH), 60.8 (CH_3), 55.6 (CH_3), 31.1 (CH_2), 10.4 (CH_3).

1-(2,3-Dimethoxyphenyl)-1-butanol.[21] Yield: 1.4 g (82%) of crude product, colorless liquid. ^{1}H NMR ($CDCl_3$, 400 MHz): δ (ppm) = 7.03 (t, J = 8.0 Hz, 1 H), 6.94 (dd, J = 8.0, 1.6 Hz, 1 H), 6.83 (dd, J = 8.0, 1.6 Hz, 1 H), 4.92 (dd, J = 8.0, 5.5 Hz, 1 H), 3.86 (s, 3 H), 3.85 (s, 3 H), 1.77 (m, 1 H), 1.68 (m, 1 H), 1.47 (m, 1 H), 1.34 (m, 1 H), 0.93 (t, J = 7.4 Hz, 3 H). ^{13}C NMR ($CDCl_3$, 100 MHz): δ (ppm) = 152.2 (C), 145.9 (C), 138.1 (C), 123.9 (CH), 118.5 (CH), 111.1 (CH), 69.6 (CH), 60.8 (CH_3), 55.6 (CH_3), 40.5 (CH_2), 19.2 (CH_2), 14.0 (CH_3). IR (KBr): ν (cm^{-1}) = 3414, 2957, 1478, 1270, 1064, 1010, 752. MS (EI): m/z = 210 [$M^{+\bullet}$], 167.

1-(2,3-Dimethoxyphenyl)-1-pentanol.[38] Yield: 1.53 g (85%) of crude product, colorless liquid. ^{1}H NMR ($CDCl_3$, 300 MHz): δ (ppm) = 7.05 (t, J = 7.9 Hz, 1 H), 6.95 (dd, J = 7.9, 1.5 Hz, 1 H), 6.84 (dd, J = 7.9, 1.5 Hz, 1 H), 4.92 (dd, J = 7.7, 5.7 Hz, 1 H), 3.87 (2 s, 3 H each), 1.76 (m, 2 H), 1.36 (m, 4 H), 0.90 (t, J = 7.4 Hz, 3 H). ^{13}C NMR ($CDCl_3$, 75 MHz): δ (ppm) = 152.5 (C), 146.2 (C), 138.3 (C), 124.1 (CH), 118.7 (CH), 111.3 (CH), 70.1 (CH), 60.9 (CH_3), 55.7 (CH_3), 38.0 (CH_2), 28.2 (CH_2), 22.6 (CH_2), 14.0 (CH_3). IR (KBr): ν (cm^{-1}) = 3415, 2934, 1479, 1268, 1009. MS (EI): m/z = 224 [$M^{+\bullet}$], 167.

1-(2,3-Dimethoxyphenyl)-1-hexanol. Yield: 1.3 g (68%) of crude product, colorless liquid. ^{1}H NMR ($CDCl_3$, 300 MHz): δ (ppm) = 7.03 (t, J = 7.9 Hz, 1 H), 6.95 (dd, J = 7.9, 1.5 Hz, 1 H), 6.82 (dd, J = 7.9, 1.5 Hz, 1 H), 4.91 (dd, J = 7.7, 5.7 Hz, 1 H), 3.87 (2 s, 3 H each), 1.73 (m, 2 H), 1.43 (m, 1 H), 1.30 (m, 5 H), 0.88 (t, J = 7.4 Hz, 3 H). ^{13}C NMR ($CDCl_3$, 75 MHz): δ (ppm) = 152.4 (C), 146.2 (C), 138.4 (C), 124.1 (CH), 118.7 (CH), 111.3 (CH), 69.9 (CH), 60.9 (CH_3), 55.7 (CH_3), 38.4 (CH_2), 31.8 (CH_2), 25.8 (CH_2), 22.5 (CH_2), 14.1 (CH_3). IR (KBr): ν (cm^{-1}) = 3415, 2933, 2860, 1477, 1268, 1072, 1010, 751. MS (EI): m/z = 238 [$M^{+\bullet}$], 167.

1-(2,3-Dimethoxyphenyl)-1-heptanol. Yield: 2.0 g (quant.) of crude product, colorless liquid. ^{1}H NMR ($CDCl_3$, 400 MHz): δ (ppm) = 7.04 (t, J = 7.7 Hz, 1 H), 6.95 (dd, J = 7.7, 1.6 Hz, 1 H), 6.83 (br. d, J = 7.7 Hz, 1 H), 4.91 (dd, J = 7.7, 5.5 Hz, 1 H), 3.87 (s, 3 H), 3.86 (s, 3 H), 1.74 (m, 2 H), 1.26 (m, 8H) 0.87 (t, J = 7.1 Hz, 3 H). ^{13}C NMR ($CDCl_3$, 100 MHz): δ (ppm) = 152.2 (C), 146.0 (C), 138.1 (C), 124.0 (CH), 118.5 (CH), 111.1 (CH), 70.0 (CH), 60.8 (CH_3), 55.6 (CH_3), 38.3 (CH_2), 31.6 (CH_2), 29.2 (CH_2), 26.0 (CH_2), 22.6 (CH_2), 14.1 (CH_3).

1-(2,3-Dimethoxyphenyl)-1-octanol.[38] Yield: 1.77 g (83%) of crude product, colorless liquid. ^{1}H NMR ($CDCl_3$, 400 MHz): δ (ppm) = 7.04 (t, J = 8.0 Hz, 1 H), 6.94 (dd, J = 8.0, 1.4 Hz, 1 H), 6.83 (dd, J = 8.0, 1.4 Hz, 1 H), 4.91 (dd, J = 8.0, 5.8 Hz, 1 H), 3.86 (s, 3 H), 3.85 (s, 3 H), 1.74 (m, 2 H), 1.46 (m, 1 H), 1.28 (m, 9 H), 0.87 (t, J = 8.1 Hz, 3 H). ^{13}C NMR ($CDCl_3$, 100 MHz): δ (ppm) = 152.2 (C), 146.0 (C), 138.1 (C), 123.9 (CH), 118.5 (CH), 111.1 (CH), 69.9 (CH), 60.8 (CH_3), 55.6 (CH_3), 38.3 (CH_2), 31.8 (CH_2), 29.7 (CH_2), 29.1 (CH_2), 26.0 (CH_2), 25.7 (CH_2), 14.1 (CH_3). IR (KBr): ν (cm^{-1}) = 3414, 2927, 2854, 1479, 1268, 1010. MS (EI): m/z = 266 [$M^{+\bullet}$], 167.

1-(2,3-Dimethoxyphenyl)-1-nonanol.[39] Yield: 1.88 g (84%) of crude product, colorless liquid. ^{1}H NMR ($CDCl_3$, 300 MHz): δ (ppm) = 7.03 (t, J = 7.8 Hz, 1 H), 6.94 (dd, J = 7.8, 1.3 Hz, 1 H), 6.82 (dd, J = 7.8, 1.3 Hz, 1 H), 4.91 (dd, J = 7.9, 5.7 Hz, 1 H), 3.85 (s, 3 H), 3.84 (s, 3 H), 1.75 (m, 2 H), 1.46 (m, 1 H), 1.28 (m, 11 H), 0.87 (m, 3 H). ^{13}C NMR ($CDCl_3$, 75 MHz): δ (ppm) = 152.5 (C), 146.2 (C), 138.4 (C), 124.1 (CH), 118.7 (CH), 111.3 (CH), 70.0 (CH), 60.8 (CH_3), 55.7 (CH_3), 38.4 (CH_2), 31.8 (CH_2), 29.7 (CH_2), 29.6 (CH_2), 29.3 (CH_2), 26.1 (CH_2), 22.7 (CH_2), 14.1 (CH_3). IR (KBr): ν (cm^{-1}) = 3409, 2926, 2854, 1479, 1268, 1009. MS (EI): m/z = 280 [$M^{+\bullet}$], 167.

1-(2,3-Dimethoxyphenyl)-1-undecanol.[38] Yield: 2.6 g (quant.) of crude product, colorless liquid. ^{1}H NMR ($CDCl_3$, 400 MHz): δ (ppm) = 7.05 (t, J = 7.9 Hz, 1 H), 6.94 (dd, J = 7.9, 1.4 Hz, 1 H), 6.84 (dd, J = 7.9, 1.4 Hz, 1 H), 4.91 (dd, J = 8.0, 5.8 Hz, 1 H), 3.87 (s, 3 H), 3.86 (s, 3 H), 1.74 (m, 2 H), 1.47 (m, 1 H), 1.26 (m, 15 H), 0.87 (m, 3 H). ^{13}C NMR ($CDCl_3$, 100 MHz): δ (ppm) = 152.3 (C), 146.0 (C), 138.0 (C), 123.9 (CH), 118.5 (CH), 111.2 (CH), 70.2 (CH), 60.8 (CH_3), 55.7 (CH_3), 38.3 (CH_2), 29.6 (3 × CH_2), 29.5 (CH_2), 29.3 (CH_2), 26.0

(37) For example, see: (a) Smith, H. E.; Russel, C. R.; Schniepp, L. E. *J. Am. Chem. Soc.* **1951**, *73*, 793−795. (b) Kaufman, T. S. *Tetrahedron Lett.* **1996**, *37*, 5329−5332.
(38) Kurtz, P. A.; Dawson, C. R. *J. Med. Chem.* **1971**, *14*, 729−732.
(39) Brown, D. G.; Hughes, W. J. J. *Z. Naturforsch., B: Chem. Sci.* **1979**, *34B*, 1408−1412.

(CH_2), 22.7 (CH_2), 14.1 (CH_3). IR (KBr): ν (cm^{-1}) = 2924, 2852, 1477, 1266, 1010, 757. MS (EI): m/z = 308 [$M^{+\bullet}$], 167.

1-(2,3-Dimethoxyphenyl)-1-tridecanol.[38] Yield: 1.5 g (56%) of crude product as colorless liquid. ^{1}H NMR ($CDCl_3$, 300 MHz): δ (ppm) = 7.04 (t, J = 7.9 Hz, 1 H), 6.95 (dd, J = 7.9, 1.6 Hz, 1 H), 6.83 (dd, J = 7.9, 1.6 Hz, 1 H), 4.91 (dd, J = 7.7, 6.1 Hz, 1 H), 3.87 (s, 3 H), 3.86 (s, 3 H), 1.75 (m, 2 H), 1.25 (m, 20 H) 0.88 (t, J = 6.9 Hz, 3 H). ^{13}C NMR ($CDCl_3$, 75.4 MHz): δ (ppm) = 152.5 (C), 146.2 (C), 138.3 (C), 124.2 (CH), 118.7 (CH), 111.4 (CH), 70.2 (CH), 60.9 (CH_3), 55.7 (CH_3), 38.4 (CH_2), 31.9 (CH_2), 29.7 (4 CH_2), 29.6 (2 CH_2), 29.4 (CH_2), 26.1 (CH_2), 22.7 (CH_2), 14.1 (CH_3).

1-(2,3-Dimethoxyphenyl)-2-methyl-1-propanol. Yield: 0.3 g (18%) after chromatography with CH_2Cl_2 on silica gel, colorless liquid. ^{1}H NMR ($CDCl_3$, 300 MHz): δ (ppm) = 7.05 (t, J = 7.9 Hz, 1 H), 6.91 (dd, J = 7.9, 1.5 Hz, 1 H), 6.84 (dd, J = 7.9, 1.5 Hz, 1 H), 4.55 (d, J = 7.7 Hz, 1 H), 3.87 (s, 6 H), 1.98 (m, 1 H), 1.06 (d, J = 6.4 Hz, 3 H), 0.82 (d, J = 6.9 Hz, 3 H). ^{13}C NMR ($CDCl_3$, 75.4 MHz): δ (ppm) = 152.5 (C), 146.5 (C), 137.1 (C), 123.9 (CH), 119.7 (CH), 111.3 (CH), 76.0 (CH), 60.9 (CH_3), 55.7 (CH_3), 34.9 (CH), 19.6 (CH_3), 18.5 (CH_3). IR (KBr): ν (cm^{-1}) = 3437.6, 2960.7, 2874.3, 1585.7, 1476.3, 1432.8, 1267.4, 1220.3, 1170.9, 1071.5, 1010.6, 754.6. MS (EI): m/z = 210 [$M^{+\bullet}$], 167.

(2,3-Dimethoxyphenyl)phenylmethanol.[40] Yield: 2.40 g (quant.) of crude product, colorless oil. ^{1}H NMR ($CDCl_3$, 300 MHz): δ (ppm) = 7.35 (m, 2 H), 7.28 (m, 2 H), 7.20 (m, 1 H), 7.02 (t, J = 7.9 Hz, 1 H), 6.96 (dd, J = 7.9, 1.5 Hz, 1 H), 6.82 (dd, J = 7.9, 1.5 Hz, 1 H), 6.00 (s, 1 H), 3.79 (s, 3 H), 3.56 (s, 3 H).

General Procedure for the Oxidation of the Alcohols. Jones reagent (for 1 mmol of substrate): 100 mg of $Na_2Cr_2O_7$ are dissolved in 0.2 mL water, 136 mg of concentrated H_2SO_4 are added, and the mixture is filled up with water to 0.5 mL. The alcohol (1 mmol) is dissolved in acetone (15 mL), and at room temperature Jones reagent is added slowly. The mixture is stirred at room temperature for 3 h and filtered and 10 mL of water are added. Acetone is removed in vacuo, and the residue is extracted with 10 mL of ether (3×). The organic phase is dried over Na_2SO_4, and the solvent is removed. If necessary, the crude product can be purified by column chromatography on silica gel.

(2,3-Dimethoxyphenyl)methyl Ketone.[37,41] Yield: 405 mg (75%) of a yellow solid. ^{1}H NMR ($CDCl_3$, 300 MHz): δ (ppm) = 7.12 (t, J = 7.8 Hz, 1 H), 7.08 (dd, J = 7.8, 1.8 Hz, 1 H), 6.89 (dd, J = 7.8, 1.8 Hz, 1 H), 4.03 (s, 3 H), 3.79 (s, 3 H), 1.60 (s, 3 H).

(2,3-Dimethoxyphenyl)ethyl Ketone.[21] Yield: 120 mg (8.5%) and 0.47 g of crude product, which is purified by chromatography (ethyl acetate/hexane 1:10), colorless oil. ^{1}H NMR ($CDCl_3$, 400 MHz): δ (ppm) = 7.14 (dd, J = 7.7, 1.6 Hz, 1 H), 7.08 (t, J = 7.7 Hz, 1 H), 7.02 (dd, J = 7.7, 1.6 Hz, 1 H), 3.89 (s, 3 H), 3.88 (s, 3 H), 2.98 (q, J = 7.1 Hz, 2 H), 1.18 (t, J = 7.1 Hz, 3 H). ^{13}C NMR ($CDCl_3$, 100 MHz): δ (ppm) = 203.7 (C), 152.8 (C), 147.7 (C), 134.0 (C), 123.9 (CH), 120.4 (CH), 115.1 (CH), 61.4 (CH_3), 55.9 (CH_3), 36.5 (CH_2), 8.4 (CH_3). IR (KBr): ν (cm^{-1}) = 2975, 1938, 1686, 1580, 1474, 1427, 1308, 1266, 1239, 1004, 781. MS (EI): m/z = 194 [$M^{+\bullet}$], 165.

(2,3-Dimethoxyphenyl)propyl Ketone.[21] Yield: 0.9 g (65%) by chromatography (dichloromethane), colorless oil. ^{1}H NMR ($CDCl_3$, 400 MHz): δ (ppm) = 7.12−7.01 (m, 3 H), 3.88 (s, 6 H), 2.93 (t, J = 7.4 Hz, 2 H), 1.71 (sextet, J = 7.4 Hz, 2 H), 0.96 (t, J = 7.4 Hz, 3 H). ^{13}C NMR ($CDCl_3$, 100 MHz): δ (ppm) = 203.4 (C), 152.8 (C), 147.6 (C), 134.3 (C), 123.9 (CH), 120.3 (CH), 115.1 (CH), 61.4 (CH_3), 55.9 (CH_3), 45.3 (CH_2), 17.7 (CH_2), 13.8 (CH_3). IR (KBr): ν (cm^{-1}) = 2963, 1683, 1473, 1267, 1234, 1007. MS (EI): m/z = 208 [$M^{+\bullet}$], 165.

(2,3-Dimethoxyphenyl)butyl Ketone.[42] Yield: 350 mg (23%), colorless oil. The product was not pure after chromatography (dichloromethane). The crude product was then overoxidized, and the product could be isolated by filtration of the mixture and removal of solvent. ^{1}H NMR ($CDCl_3$, 300 MHz): δ (ppm) = 7.11−7.01 (m, 3 H), 3. 90 (s, 3 H), 3.89 (s, 3 H), 2.96 (t, J = 7.4 Hz, 2 H), 1.68 (m, 2 H), 1.38 (m, 2 H), 0.93 (t, J = 7.4 Hz, 3 H). ^{13}C NMR ($CDCl_3$, 75 MHz): δ (ppm) = 204.0 (C), 153.0 (C), 147.8 (C), 134.6 (C), 124.1 (CH), 120.5 (CH), 115.2 (CH), 61.5 (CH_3), 56.0 (CH_3), 43.2 (CH_2), 26.4 (CH_2), 22.5 (CH_2), 13.9 (CH_3). IR (KBr): ν (cm^{-1}) = 2957, 1683, 1474, 1266, 1230, 1004, 751. MS (EI): m/z = 222 [$M^{+\bullet}$], 165.

(2,3-Dimethoxyphenyl)pentyl Ketone.[41] Yield: 390 mg (31%), colorless oil by chromatography (dichloromethane). ^{1}H NMR ($CDCl_3$, 400 MHz): δ (ppm) = 7.12−7.00 (m, 3 H), 3.88 (s, 6 H), 2.94 (t, J = 7.7 Hz, 2 H), 1.68 (m, 2 H), 1.33 (m, 4 H), 0.90 (m, 3 H). ^{13}C NMR ($CDCl_3$, 100 MHz): δ (ppm) = 203.6 (C), 152.7 (C), 147.6 (C), 134.4 (C), 123.9 (CH), 120.3 (CH), 115.0 (CH), 61.4 (CH_3), 55.9 (CH_3), 43.3 (CH_2), 31.5 (CH_2), 24.0 (CH_2), 22.5 (CH_2), 14.0 (CH_3). IR (KBr): ν (cm^{-1}) = 2936, 1684, 1472, 1264, 1005. MS (EI): m/z = 236 [$M^{+\bullet}$], 165.

(2,3-Dimethoxyphenyl)hexyl Ketone.[41] Yield: 550 mg (28%) after purification by chromatography (dichloromethane), colorless oil. ^{1}H NMR ($CDCl_3$, 400 MHz): δ (ppm) = 7.09 (m, 2 H), 7.02 (dd, J = 7.4, 2.4 Hz, 1 H), 3.88 (2 s, 3 H each), 2.94 (t, J = 7.4 Hz, 2 H), 1.68 (m, 2 H), 1.30 (m, 6 H), 0.88 (t, J = 6.8 Hz, 3 H). ^{13}C NMR ($CDCl_3$, 100 MHz): δ (ppm) = 203.6 (C), 152.7 (C), 147.6 (C), 134.4 (C), 123.9 (CH), 120.3 (CH), 115.0 (CH), 61.4 (CH_3), 55.9 (CH_3), 43.4 (CH_2), 31.6 (CH_2), 29.0 (CH_2), 24.3 (CH_2), 22.5 (CH_2), 14.0 (CH_3). IR (KBr): ν (cm^{-1}) = 2930, 1474, 1266, 1238, 1004. MS (EI): m/z = 250 [$M^{+\bullet}$], 180, 165.

(2,3-Dimethoxyphenyl)heptyl Ketone.[41] Yield: 870 mg (49%) after purification by chromatography (dichloromethane), colorless oil. ^{1}H NMR ($CDCl_3$, 400 MHz): δ (ppm) = 7.12−7.00 (m, 3 H), 3.88 (2 s, 3 H each), 2.94 (t, J = 7.8 Hz, 2 H), 1.68 (m, 2 H), 1.30 (m, 8 H), 0.88 (t, J = 6.9 Hz, 3 H). ^{13}C NMR ($CDCl_3$, 100 MHz): δ (ppm) = 203.6 (C), 152.7 (C), 147.6 (C), 134.4 (C), 123.9 (CH), 120.3 (CH), 115.0 (CH), 61.4 (CH_3), 55.9 (CH_3), 43.4 (CH_2), 31.7 (CH_2), 29.6 (CH_2), 29.1 (CH_2), 24.3 (CH_2), 22.6 (CH_2), 14.1 (CH_3). IR (KBr): ν (cm^{-1}) = 2927, 2856, 1684, 1472, 1265, 1005. MS (EI): m/z = 264 [$M^{+\bullet}$], 180, 165.

(2,3-Dimethoxyphenyl)octyl Ketone. Yield: 1.01 g (61%) after purification by chromatography (dichloromethane), colorless oil. ^{1}H NMR ($CDCl_3$, 400 MHz): δ (ppm) = 7.12−7.00 (m, 3 H), 3.89 (s, 3 H), 3.88 (s, 3 H), 2.94 (t, J = 7.5 Hz, 2 H), 1.68 (m, 2 H), 1.29 (m, 10 H), 0.87 (m, 3 H). ^{13}C NMR ($CDCl_3$, 100 MHz): δ (ppm) = 203.6 (C), 152.7 (C), 147.6 (C), 134.4 (C), 123.9 (CH), 120.4 (CH), 115.0 (CH), 61.4 (CH_3), 55.9 (CH_3), 43.4 (CH_2), 31.9 (CH_2), 29.6 (CH_2), 29.4 (CH_2), 29.1 (CH_2), 24.3 (CH_2), 22.6 (CH_2), 14.1 (CH_3). IR (KBr): ν (cm^{-1}) = 2926, 2855, 1684, 1471, 1264. MS (EI): m/z = 278 [$M^{+\bullet}$], 180, 165.

(2,3-Dimethoxyphenyl)decyl Ketone. Yield: 1.0 g (40%) after purification by chromatography (dichloromethane), colorless oil. ^{1}H NMR ($CDCl_3$, 400 MHz): δ (ppm) = 7.12−7.00 (m, 3 H), 3.89 (s, 3 H), 3.88 (s, 3 H), 2.94 (t, J = 7.1 Hz, 2 H), 1.68 (m, 2 H), 1.29 (m, 14 H), 0.88 (t, J = 7.1 Hz, 3 H). ^{13}C NMR ($CDCl_3$, 100 MHz): δ (ppm) = 203.6 (C), 152.7 (C), 147.6 (C), 134.4 (C), 123.9 (CH), 120.3 (CH), 115.0 (CH), 61.4 (CH_3), 55.9 (CH_3), 43.4 (CH_2), 31.9 (CH_2), 29.6 (CH_2), 29.5 (2 × CH_2), 29.4 (CH_2), 29.1 (CH_2), 24.3 (CH_2), 22.7 (CH_2), 14.1 (CH_3). IR (KBr): ν (cm^{-1}) = 2926, 2853, 1683, 1473, 1266, 1234, 1006. MS (EI): m/z = 306 [$M^{+\bullet}$], 180, 165.

(2,3-Dimethoxyphenyl)dodecyl Ketone. Yield: 0.8 mg (53%) after purification by chromatography (ethyl acetate/hexane 1:10), colorless oil. ^{1}H NMR ($CDCl_3$, 300 MHz): δ (ppm) = 7.09 (m, 2 H), 7.03 (dd, J = 6.9, 3.0 Hz, 1 H), 3.90 (s, 3 H), 3.89 (s, 3 H), 2.95 (t, J = 7.2 Hz, 2 H), 1.68 (m, 2 H), 1.26 (m, 18 H), 0.89 (t, J = 6.9 Hz, 3 H). ^{13}C NMR ($CDCl_3$, 100 MHz): δ (ppm) = 204.0 (C), 152.6 (C), 147.8 (C), 134.6 (C), 124.1 (CH), 120.5 (CH), 115.2 (CH), 61.6 (CH_3), 56.0 (CH_3), 43.5 (CH_2), 31.9 (CH_2), 29.7 (CH_2), 29.6 (2 CH_2), 29.5 (2 CH_2), 29.3 (2 CH_2), 24.3 (CH_2), 22.7 (CH_2), 14.1 (CH_3). IR (KBr): ν (cm^{-1}) =

(40) Boehme, W. R.; Scharpf, W. G. *J. Org. Chem.* **1961**, *26*, 1692−1695.

2925, 2853, 1683, 1472, 1265, 1234, 1006, 751. MS (EI): m/z = 334 [$M^{+\bullet}$], 180, 165.

2,3-Dimethoxyphenyl)isopropyl Ketone. Yield: 270 mg (60%) after purification by chromatography (dichloromethane), colorless oil. ^{1}H NMR ($CDCl_3$, 300 MHz): δ (ppm) = 7.10−6.95 (m, 3 H), 3.89 (s, 3 H), 3.86 (s, 3 H), 3.36 (sept., J = 7.9 Hz, 1 H), 1.16 (d, J = 7.9 Hz, 6 H). ^{13}C NMR ($CDCl_3$, 75.4 MHz): δ (ppm) = 208.6 (C), 152.8 (C), 147.1 (C), 134.8 (C), 124.2 (CH), 120.3 (CH), 114.7 (CH), 61.7 (CH_3), 56.0 (CH_3), 40.3 (CH), 18.5 (CH_3). IR (KBr): ν (cm^{-1}) = 2970, 1691, 1471, 1263, 1002, 754. MS (EI): m/z = 208 [$M^{+\bullet}$], 165.

2,3-Dimethoxybenzophenone.[43] Yield: 1.5 g (63%), colorless oil. ^{1}H NMR ($CDCl_3$, 400 MHz): δ (ppm) = 7.83 (m, 2 H), 7.55 (m, 1 H), 7.43 (m, 2 H), 7.12 (t, J = 7.7 Hz, 1 H), 7.05 (dd, J = 7.7, 1.6 Hz, 1 H), 6.92 (dd, J = 7.7, 1.6 Hz, 1 H), 3.90 (s, 3 H), 3.71 (s, 3 H). ^{13}C NMR ($CDCl_3$, 100 MHz): δ (ppm) = 196.0 (C), 152.5 (C), 146.7 (C), 137.3 (C), 134.0 (C), 133.0 (CH), 129.7 (CH), 128.1 (CH), 123.8 (CH), 120.3 (CH), 114.1 (CH), 61.5 (CH_3), 55.8 (CH_3). IR (KBr): ν (cm^{-1}) = 2938, 1669, 1474, 1316, 1270, 712. MS (EI): m/z = 242 [$M^{+\bullet}$], 165, 151.

General Procedure for the Deprotection of the Methyl Ethers. At 0 °C, BBr_3 (6 mmol) is added to the dimethoxyphenyl derivative (1 mmol) in 20 mL of dichloromethane. The mixture is stirred overnight at room temperature. Methanol is then added to the mixture at 0 °C. The solvent is removed in vacuo, and the residue is dissolved in ethyl acetate, washed with water, and dried with Na_2SO_4. The solvent is evaporated in vacuo again.

(2,3-Dihydroxyphenyl)methyl Ketone (5a-H$_2$).[44] Yield: 228 mg (quant.), green solid. Mp = 141 °C. ^{1}H NMR (DMSO-d_6, 400 MHz): δ (ppm) = 12.01 (s, 1 H), 9.40 (s, 1 H), 7.35 (dd, J = 8.0, 1.7 Hz, 1 H), 7.05 (dd, J = 8.0, 1.7 Hz, 1 H), 6.77 (t, J = 8.0 Hz, 1 H), 2.62 (s, 3 H). IR (KBr): ν (cm^{-1}) = 3280, 1634, 1584, 1472, 1434, 1387, 1320, 1255, 1178, 1085, 1026, 897, 826, 790, 738, 677, 617. Anal. Calcd for $C_8H_8O_3$: C, 63.16; H, 5.30. Found: C, 62.99; H, 5.44.

(2,3-Dihydroxyphenyl)ethyl Ketone (5b-H$_2$).[21] Yield: 80 mg (78%), brown solid. Mp = 56 °C. ^{1}H NMR ($CDCl_3$, 300 MHz): δ (ppm) = 12.58 (s, OH), 7.32 (dd, J = 8.1, 1.5 Hz, 1 H), 7.12 (dd, J = 8.1, 1.5 Hz, 1 H), 6.82 (t, J = 8.1 Hz, 1 H), 5.77 (br., OH), 3.05 (q, J = 7.1 Hz, 2 H), 1.25 (t, J = 7.1 Hz, 3 H). ^{13}C NMR ($CDCl_3$, 75.4 MHz): δ (ppm) = 207.7 (C), 149.5 (C), 145.5 (C), 120.6 (CH), 120.1 (CH), 119.1 (C), 118.9 (CH), 31.7 (CH_2), 8.2 (CH_3). IR (KBr): ν (cm^{-1}) = 3489, 1637, 1454, 1268, 729. MS (EI): m/z = 166 [$M^{+\bullet}$], 137. Anal. Calcd for $C_9H_{10}O_3$: C, 65.05; H, 6.07. Found: C, 65.34; H, 6.43.

(2,3-Dihydroxyphenyl)propyl Ketone (5c-H$_2$).[21] Yield: 500 mg (91%), brown solid. Mp = 59 °C. ^{1}H NMR ($CDCl_3$, 400 MHz): δ (ppm) = 12.63 (s, OH), 7.32 (dd, J = 8.2, 1.4 Hz, 1 H), 7.12 (dd, J = 8.2, 1.4 Hz, 1 H), 6.81 (t, J = 8.2 Hz, 1 H), 5.75 (br., OH), 2.97 (t, J = 7.2 Hz, 2 H), 1.79 (sextet, J = 7.2 Hz, 2 H), 1.02 (t, J = 7.2 Hz, 3 H). ^{13}C NMR ($CDCl_3$, 100 MHz): δ (ppm) = 207.0 (C), 149.4 (C), 145.3 (C), 120.5 (CH), 119.9 (CH), 118.8 (C), 118.7 (CH), 40.3 (CH_2), 17.9 (CH_2), 13.8 (CH_3). IR (KBr): ν (cm^{-1}) = 3477, 1641, 1453, 1261, 1206, 830, 745, 570. MS (EI): m/z = 180 [$M^{+\bullet}$], 137. Anal. Calcd for $C_{10}H_{12}O_3$: C, 66.65; H, 6.71. Found: C, 65.96; H, 7.20.

(2,3-Dihydroxyphenyl)butyl Ketone (5d-H$_2$). Yield: 200 mg (68%), brown solid. Mp = 50 °C. ^{1}H NMR ($CDCl_3$, 400 MHz): δ (ppm) = 12.63 (s, OH), 7.32 (dd, J = 8.2, 1.4 Hz, 1 H), 7.12 (dd, J = 8.2, 1.4 Hz, 1 H), 6.81 (t, J = 8.2 Hz, 1 H), 5.75 (br., OH), 2.99 (t, J = 7.7 Hz, 2 H), 1.73 (m, 2 H), 1.42 (m, 2 H), 0.97 (t, J = 7.4 Hz, 3 H). ^{13}C NMR ($CDCl_3$, 100 MHz): δ (ppm) = 207.2 (C), 149.4 (C), 145.3 (C), 120.5 (CH), 119.9 (CH), 119.0 (C), 118.7 (CH), 38.1 (CH_2), 26.6 (CH_2), 22.4 (CH_2), 13.9 (CH_3). IR (KBr): ν (cm^{-1}) = 3355, 2958, 1634, 1383, 1279, 1057, 730. MS (EI): m/z = 194 [$M^{+\bullet}$], 137.

(2,3-Dihydroxyphenyl)pentyl Ketone (5e-H$_2$). Yield: 300 mg (87%), brown solid. Mp = 52 °C. ^{1}H NMR ($CDCl_3$, 400 MHz): δ (ppm) = 12.63 (s, OH), 7.32 (dd, J = 8.2, 1.4 Hz, 1 H), 7.12 (dd, J = 8.2, 1.4 Hz, 1 H), 6.81 (t, J = 8.2 Hz, 1 H), 5.74 (br., OH), 2.98 (t, J = 7.3 Hz, 2 H), 1.75 (m, 2 H), 1.38 (m, 4 H), 0.92 (t, J = 7.2 Hz, 3 H). ^{13}C NMR ($CDCl_3$, 100 MHz): δ (ppm) = 207.2 (C), 149.4 (C), 145.3 (C), 120.5 (CH), 119.8 (CH), 119.0 (C), 118.7 (CH), 38.4 (CH_2), 31.4 (CH_2), 24.2 (CH_2), 22.4 (CH_2), 13.9 (CH_3). IR (KBr): ν (cm^{-1}) = 3359, 2934, 2683, 1635, 1456, 1383, 1276, 1059. MS (EI): m/z = 208 [$M^{+\bullet}$], 137. Anal. Calcd for $C_{12}H_{16}O_3 \cdot {}^1/_4H_2O$: C, 67.74; H, 7.82. Found: C, 67.85; H, 8.12.

(2,3-Dihydroxyphenyl)hexyl Ketone (5f-H$_2$). Yield: 300 mg (70%), brown solid. Mp = 46 °C. ^{1}H NMR ($CDCl_3$, 300 MHz): δ (ppm) = 12.63 (s, OH), 7.32 (dd, J = 8.1, 1.5 Hz, 1 H), 7.12 (dd, J = 8.1, 1.5 Hz, 1 H), 6.81 (t, J = 8.1 Hz, 1 H), 5.72 (br., OH), 2.98 (t, J = 7.2 Hz, 2 H), 1.74 (m, 2 H), 1.34 (m, 6 H), 0.90 (t, J = 7.0 Hz, 3 H). ^{13}C NMR ($CDCl_3$, 75 MHz): δ (ppm) = 207.5 (C), 149.7 (C), 145.6 (C), 120.7 (CH), 120.1 (CH), 119.2 (C), 118.9 (CH), 38.5 (CH_2), 31.6 (CH_2), 29.0 (CH_2), 24.5 (CH_2), 22.5 (CH_2), 14.0 (CH_3). IR (KBr): ν (cm^{-1}) = 3352, 2956, 2926, 1635, 1456, 1272, 1234, 728. MS (EI): m/z = 222 [$M^{+\bullet}$], 137. Anal. Calcd for $C_{13}H_{18}O_3$: C, 70.24; H, 8.16. Found: C, 69.66; H, 8.30.

(2,3-Dihydroxyphenyl)heptyl Ketone (5g-H$_2$). Yield: 320 mg (71%), brown solid. Mp = 47 °C. ^{1}H NMR ($CDCl_3$, 300 MHz): δ (ppm) = 12.63 (s, OH), 7.31 (dd, J = 8.2, 1.5 Hz, 1 H), 7.12 (dd, J = 8.2, 1.5 Hz, 1 H), 6.81 (t, J = 8.2 Hz, 1 H), 5.76 (br., OH), 2.98 (t, J = 7.6 Hz, 2 H), 1.74 (m, 2 H), 1.40−1.26 (m, 8 H), 0.89 (m, 3 H). ^{13}C NMR ($CDCl_3$, 75 MHz): δ (ppm) = 207.5 (C), 149.7 (C), 145.6 (C), 120.7 (CH), 120.0 (CH), 119.2 (C), 118.9 (CH), 38.5 (CH_2), 31.7 (CH_2), 29.3 (CH_2), 29.1 (CH_2), 24.5 (CH_2), 22.6 (CH_2), 14.1 (CH_3). IR (KBr): ν (cm^{-1}) = 3360, 2923, 1624, 1457, 1232, 895, 727. MS (EI): m/z = 236 [$M^{+\bullet}$], 137. Anal. Calcd for $C_{14}H_{20}O_3 \cdot {}^1/_4$ H_2O: C, 69.83; H, 8.58. Found: C, 70.08; H, 8.80.

(2,3-Dihydroxyphenyl)octyl Ketone (5h-H$_2$). Yield: 500 mg (80%), brown solid. Mp = 41 °C. ^{1}H NMR ($CDCl_3$, 300 MHz): δ (ppm) = 12.64 (s, OH), 7.32 (m, 1 H), 7.12 (m, 1 H), 6.82 (m, 1 H), 5.75 (br., OH), 2.99 (t, J = 7.2 Hz, 2 H), 1.75 (m, 2 H), 1.38−1.25 (m, 10 H), 0.89 (m, 3 H). ^{13}C NMR ($CDCl_3$, 75 MHz): δ (ppm) = 207.5 (C), 149.7 (C), 145.5 (C), 120.7 (CH), 120.0 (CH), 119.2 (C), 118.9 (CH), 38.5 (CH_2), 31.9 (CH_2), 29.7 (CH_2), 29.4 (CH_2), 29.1 (CH_2), 24.5 (CH_2), 22.7 (CH_2), 14.1 (CH_3). IR (KBr): ν (cm^{-1}) = 2924, 2855, 1637, 1458, 1277. MS (EI): m/z = 250 [$M^{+\bullet}$], 137. Anal. Calcd for $C_{14}H_{20}O_3$: C, 71.97; H, 8.86. Found: C, 73.42; H, 8.85.

(2,3-Dihydroxyphenyl)decyl Ketone (5i-H$_2$). Yield: 625 mg (86%), brown solid. Mp = 52 °C. ^{1}H NMR ($CDCl_3$, 400 MHz): δ (ppm) = 12.63 (s, OH), 7.32 (dd, J = 8.2, 1.4 Hz, 1 H), 7.11 (m, 1 H), 6.81 (t, J = 8.2 Hz, 1 H), 5.74 (br., OH), 2.98 (t, J = 7.4 Hz, 2 H), 1.74 (m, 2 H), 1.41−1.25 (m, 14 H), 0.88 (t, J = 7.1 Hz, 3 H). ^{13}C NMR ($CDCl_3$, 100 MHz): δ (ppm) = 207.2 (C), 149.4 (C), 145.3 (C), 120.5 (CH), 119.8 (CH), 119.0 (C), 118.7 (CH), 38.4 (CH_2), 31.8 (CH_2), 29.7 (CH_2), 29.5 (CH_2), 29.4 (2 × CH_2), 29.3 (CH_2), 24.5 (CH_2), 22.7 (CH_2), 14.1 (CH_3). IR (KBr): ν (cm^{-1}) = 3355, 2920, 2850, 1635, 1456, 728. MS (EI): m/z = 278 [$M^{+\bullet}$], 137. Anal. Calcd for $C_{17}H_{26}O_3$: C, 73.35; H, 9.41. Found: C, 72.75; H, 8.71.

(2,3-Dihydroxyphenyl)dodecyl Ketone (5j-H$_2$). Yield: 560 mg (79%), brown solid. Mp = 60 °C. ^{1}H NMR ($CDCl_3$, 400 MHz): δ (ppm) = 12.63 (s, OH), 7.32 (dd, J = 8.2, 1.4 Hz, 1 H), 7.12 (dd, J = 8.2, 1.4 Hz, 1 H), 6.81 (t, J = 8.2 Hz, 1 H), 5.72 (br., OH), 2.98 (t, J = 7.4 Hz, 2 H), 1.74 (m, 2 H), 1.26 (m, 18 H), 0.88 (t, J = 7.1 Hz, 3 H). ^{1}H NMR (methanol-d_4, 300 MHz): δ (ppm) = 7.38 (dd, J = 8.1, 1.5 Hz, 1 H), 7.02 (dd, J = 8.1, 1.5 Hz, 1 H), 6.78 (t, J = 8.2 Hz, 1 H), 3.02 (t, J = 7.4 Hz, 2 H), 1.72 (m, 2 H), 1.29 (m, 18 H), 0.89 (t, J = 7.1 Hz, 3 H). IR (KBr): ν (cm^{-1}) = 2918, 2850, 1635, 1456,

(41) Tsatsas, G.; Guioka-Dedopoulou, V. *Bull. Chim. Soc. Fr.* **1964**, 2610−2612.
(42) Schildknecht, H.; Schmidt, H. *Z. Naturforsch., B: Chem. Sci.* **1967**, *22B*, 287−294.
(43) Richtzenhain, H.; Nippus, P. *Chem. Ber.* **1949**, *82*, 408−417.
(44) Ghosh, S. K.; Bose, R. N.; Gould, E. S. *Inorg. Chem.* **1988**, *27*, 1620−1625.

1276, 1239, 728. MS (EI): $m/z = 306$ [$M^{+\bullet}$], 288, 189, 165, 152, 137. Anal. Calcd for $C_{19}H_{30}O_3$: C, 74.47; H, 9.87. Found: C, 74.36; H, 9.94.

(2,3-Dihydroxyphenyl)isopropyl Ketone (6a-H$_2$). Yield: 80 mg (62%), brown wax. ^{1}H NMR ($CDCl_3$, 300 MHz): δ (ppm) = 12.77 (s, OH), 7.34 (dd, $J = 8.2$, 1.5 Hz, 1 H), 7.13 (dd, $J = 8.2$, 1.5 Hz, 1 H), 6.82 (t, $J = 8.2$ Hz, 1 H), 5.80 (br., OH), 3.58 (sept., $J = 7.1$ Hz, 1 H), 1.25 (d, $J = 7.1$ Hz, 6 H). ^{13}C NMR ($CDCl_3$, 75.4 MHz): δ (ppm) = 211.3 (C), 150.3 (C), 145.7 (C), 120.6 (CH), 120.0 (CH), 118.8 (CH), 118.0 (C), 35.2 (CH), 19.2 (CH_3). IR (KBr): ν (cm^{-1}) = 2976, 1637, 1452, 1269, 755. MS (EI): $m/z = 181$ [MH^+], 180 [$M^{+\bullet}$], 137.

2,3-Dihydroxybenzophenone (6b-H$_2$).[45] Yield: 880 mg (quant). ^{1}H NMR ($CDCl_3$, 300 MHz): δ (ppm) = 12.23 (s, OH), 7.71 (m, 2 H), 7.59 (m, 1 H), 7.51 (m, 2 H), 7.16 (m, 2 H), 7.13 (dd, $J = 8.2$, 1.5 Hz, 1 H), 6.80 (t, $J = 7.9$ Hz, 1 H), 5.82 (br., OH). − ^{13}C NMR ($CDCl_3$, 75.4 MHz,): δ (ppm) = 201.8 (C), 150.2 (C), 145.6 (C), 137.7 (C), 132.1 (CH), 129.2 (CH), 128.3 (CH), 124.5 (CH), 120.4 (CH), 119.0 (C), 118.7 (CH). IR (KBr): ν (cm^{-1}) = 3383, 1623, 1449, 1326, 1260, 730. MS (EI): $m/z = 215$ [MH^+], 214 [$M^{+\bullet}$], 136. Anal. Calcd for $C_{13}H_{10}O_3 \cdot {}^1/_4H_2O$: C, 71.39; H, 4.84. Found: C, 71.63; H, 5.14.

2,3-Dihydroxybenzoicacid Methylester (7a-H$_2$). **7a**-H_2 was prepared as described in the literature.[22]

2,3-Dihydroxybenzoicacid Ethylester (7b-H$_2$).[46] 2,3-Dihydroxybenzoicacid (0.01 mol) and $SOCl_2$ (15 mL) are dissolved in $CHCl_3$ (50 mL). The mixture is refluxed under N_2 overnight. The solvent is removed, and the residue is dissolved in CH_2Cl_2 and under ice cooling slowly is added to a mixture of ethanol and CH_2Cl_2. After stirring overnight and removal of the solvent, the ester is obtained in 68% yield. Mp = 64 °C. ^{1}H NMR (300 MHz, $CDCl_3$): δ (ppm) = 11.01 (s, 1 H), 7.39 (dd, $J = 1.5$, 7.8 Hz, 1 H), 7.11 (dd, $J = 1.5$, 7.8 Hz, 1 H), 6.80 (t, $J = 7.8$ Hz, 1 H), 5.70 (s, 1 H), 4.43 (q, $J = 7.2$ Hz, 2 H), 1.43 (t, $J = 7.2$ Hz, 3 H). ^{13}C NMR (100 MHz, $CDCl_3$): δ (ppm) = 170.5 (C), 149.0 (C), 144.9 (C), 120.6 (CH), 119.7 (CH), 119.1 (CH), 112.4 (C), 61.6 (CH_2), 14.2 (CH_2). IR (KBr): ν (cm^{-1}) = 3476, 1674, 1465, 1312, 1271, 1154, 759. MS (EI): $m/z = 182$ [$M^{+\bullet}$], 136.

General Procedure for the Preparation of Metal Complexes. 2,3-Dihydroxyaryl ketone (1 equiv, approx 0.7 mmol), titanyl bis(acetylacetonate) (1 equiv), and lithium carbonate (1 equiv) are dissolved in DMF (30 mL), and the solution is stirred overnight. The solvent is removed, and the residue is dried in vacuo. The complexes are obtained in quantitative yield as a red solid. Yellow gallium complexes were analogously prepared from $Ga(acac)_3$ in the presence of 1.5 equiv of Li_2CO_3.

Li$_2$[Ti(4)$_3$]/Li$_4$[Ti$_2$(4)$_6$]. ^{1}H NMR (CD_3OD, 300 MHz): monomer (major component) δ (ppm) = 10.20 (s, 3H), 6.97 (dd, $J = 6.4$, 2.5 Hz, 3 H), 6.59−6.51 (m, 6 H); dimer (minor component) δ (ppm) = 8.74 (s, 6 H), 6.89 (dd, $J = 7.7$, 1.4 Hz, 6 H), 6.77 (t, $J = 7.7$ Hz, 6 H), 6.59−6.51 (m, 6 H). ^{13}C NMR (DMSO-d_6, 75 MHz): only monomer δ (ppm) = 162.8 (CH), 161.3 (C), 153.3 (C), 118.8 (C), 116.9 (CH), 114.0 (CH), 113.1 (CH). IR (KBr): ν (cm^{-1}) = 1663, 1592, 1550, 1449, 1406, 1253, 1206, 747, 668, 592, 528. Anal. Calcd for $C_{21}H_{12}Li_2O_9Ti \cdot 2\ C_3H_7NO \cdot 2\ H_2O$: C, 49.71; H, 4.64; N, 4.29. Found: C, 50.02; H, 4.44; N, 4.45. Negative ESI FTICR-MS (THF): $m/z = 933$ [Li_3(**4**)$_6Ti_2$]$^-$, 463 [Li(**4**)$_3$Ti]$^-$, 457 [H(**4**)$_3$Ti]$^-$.

X-ray Crystallographic Study of Li$_4$[Ti$_2$(4)$_6$]: The data set was collected with a Nonius KappaCCD diffractometer, equipped with a rotating anode generator. Programs used: data collection COLLECT (Nonius B. V., 1998), data reduction Denzo-SMN,[47] structure solution SHELXS-97,[48] structure refinement SHELXL-97 (G. M. Sheldrick, Universität Göttingen, 1997), graphics SCHAKAL (E. Keller, Universität Freiburg, 1997)(Table 3).

Li$_3$[Ga(4)$_3$]/Li$_6$[Ga$_2$(4)$_6$]. ^{1}H NMR (DMSO-d_6, 300 MHz): monomer (major component) δ (ppm) = 10.06 (s, 3 H), 6.49 (dd, $J = 8.2$, 1.7 Hz, 3 H), 6.35−6.27 (m, 6 H); dimer (minor component) δ (ppm) = 8.53 (s, 6 H), 6.35−6.27 (m, 12 H), 6.12 (t, $J = 7.7$ Hz, 3 H). ^{13}C NMR (DMSO-d_6, 75 MHz, only monomer is observed): δ (ppm) = 191.3 (CH), 159.2 (C), 157.3 (C), 120.3 (C), 118.4 (CH), 115.3 (CH), 114.9 (CH). IR (KBr): ν (cm^{-1}) = 3412, 1658, 1588, 1545, 1446, 1412, 1255, 789, 659, 532. Anal. Calcd for $(C_{42}H_{24}Li_6O_{18}Ga) \cdot 2C_3H_7NO \cdot 4\ H_2O$: C, 47.41; H, 3.81; N, 2.30. Found: C, 47.52; H, 3.98; N, 2.49. Negative ESI FTICR-MS (THF): $m/z = 492$ [Li_4(**4**)$_6Ga_2$]$^{2-}$, 326 [Li_3(**4**)$_6Ga_2$]$^{3-}$.

Li$_2$[(5a)$_3$Ti]/Li$_4$[(5a)$_6$Ti$_2$]. ^{1}H NMR (400 MHz, methanol-d_4): monomer (minor component) δ (ppm) = 6.99 (m, 3 H), 6.45 (m, 6 H), 2.61 (s, 9 H); dimer (major component) δ (ppm) = 7.10 (m, 6 H), 6.56 (m, 12 H), 1.87 (s, 18 H). IR (drift, KBr): ν (cm^{-1}) = 3429, 1654, 1592, 1430, 1294, 1255, 1217, 910, 844, 717, 534. Anal. Calcd for $C_{48}H_{36}Li_4O_{18}Ti_2 \cdot 4\ C_3H_7NO \cdot 9\ H_2O$: C, 48.73; H, 5.59; N, 3.79. Found: C, 48.43; H, 5.19; N, 3.64. Negative ESI FTICR-MS (THF): $m/z = 1017$ [Li_3(**5a**)$_6Ti_2$]$^-$, 505 [Li(**5a**)$_3$Ti]$^-$.

Li$_3$[(5a)$_3$Ga]/Li$_6$[(5a)$_6$Ga$_2$]. ^{1}H NMR (DMSO-d_6, 400 MHz): monomer (minor component) δ (ppm) = 6.80−6.70 (m, 3 H), 6.53−6.44 (m, 3H), 6.22−6.19 (m, 3 H), 2.60 (br, 3 H); dimer (major component) δ (ppm) = 6.59 (d, $J = 8.0$ Hz, 6 H), 6.30 (d, $J = 8.0$ Hz, 6 H), 6.14 (t, $J = 8.0$ Hz, 6H), 1.74 (s, 18 H). IR (KBr): ν (cm^{-1}) = 3456, 1651, 1592, 1552, 1439, 1305, 1269, 1220, 906, 734, 705. Anal. Calcd for $C_{48}H_{36}Li_6O_{18}Ga_2 \cdot 3\ C_3H_7NO \cdot 9\ H_2O$: C, 46.79; H, 5.17; N, 2.87. Found: C, 46.51; H, 4.77; N, 2.90. Negative ESI FTICR-MS (THF): $m/z = 534$ [Li_4(**4**)$_6Ga_2$]$^{2-}$, 354 [Li_3(**4**)$_6Ga_2$]$^{3-}$.

Li$_2$[(5b)$_3$Ti]/Li$_4$[(5b)$_6$Ti$_2$]. ^{1}H NMR (methanol-d_4, 400 MHz): monomer (minor component) δ (ppm) = 6.96 (dd, $J = 7.3$, 2.8 Hz, 3 H), 6.46 (m, 6 H), 3.11 (q, $J = 7.4$ Hz, 6 H), 1.05 (t, $J = 7.4$ Hz, 9 H); dimer (major component) δ (ppm) = 7.10 (dd, $J = 6.1$, 3.8 Hz, 6 H), 6.56 (m, 12 H), 2.72 (m, 6 H), 2.12 (m, 6 H), 0.47 (t, $J = 7.2$ Hz, 18 H). Negative ESI FTICR-MS (THF): $m/z = 1117$ [$NaLi_2$(**L**)$_6Ti_2$]$^-$, 1101 [Li_3(**L**)$_6Ti_2$]$^-$, 547 [Li(**L**)$_3$Ti]$^-$. IR (KBr): ν (cm^{-1}) = 3447, 2930, 1655, 1432, 1259, 1216, 885, 738. − Calcd. for $C_{27}H_{24}O_9TiLi_2 \cdot 9\ H_2O$: C 45.27, H 5.91; found: C 44.83, H 5.49. Negative ESI FTICR-MS (THF): $m/z = 1117$ [$NaLi_2$(**5b**)$_6Ti_2$]$^-$, 1101 [Li_3(**5b**)$_6Ti_2$]$^-$, 547 [Li(**5b**)$_3$Ti]$^-$.

X-ray Crystallographic Study of Li$_4$[(5b)$_6$Ti$_2$]: The data set was collected on an Enraf-Nonius CAD4 diffractometer employing graphite-monochromated Cu Kα radiation ($\lambda = 1.541\ 79$ Å). The structure has been solved by direct methods as implemented in the Xtal3.7 suite of crystallographic routines [49] where GENSIN has been used to generate the structure-invariant relationships and CRISP for the tangent phasing procedure.

Li$_2$[(5c)$_3$Ti]/Li$_4$[(5c)$_6$Ti$_2$]. ^{1}H NMR (methanol-d_4, 400 MHz): monomer (minor component) δ (ppm) = 6.98 (dd, $J = 8.0$, 2.2 Hz, 3 H), 6.48 (dd, $J = 8.0$, 2.2 Hz, 3 H), 6.44 (t, $J = 8.0$ Hz, 3 H), 3.06 (t, $J = 7.4$ Hz, 6 H), 1.59 (sextet, $J = 7.4$ Hz, 6 H), 0.85 (t, $J = 7.4$ Hz, 9 H); dimer (major component) δ (ppm) = 7.11 (dd, $J = 6.3$, 3.6 Hz, 6 H), 6.58 (m, 12 H), 2.68 (m, 6 H), 1.96 (m, 6 H), 1.10 (m, 6 H), 0.98 (m, 6 H), 0.63 (t, $J = 7.7$ Hz, 18 H). ^{13}C NMR (methanol-d_4, 100 MHz, only dimer is observed): dimer δ (ppm) = 201.3 (C), 159.9 (C), 159.4 (C), 120.9 (CH), 120.2 (C), 117.2 (CH), 115.9 (CH), 40.5 (CH_2), 17.3 (CH_2), 12.6 (CH_3). IR (KBr): ν (cm^{-1}) = 3427, 2960, 1656, 1429, 1258, 1214, 536. Negative ESI FTICR-MS (THF): $m/z = 1185$ [Li_3(**5c**)$_6Ti_2$]$^-$, 589 [Li(**5c**)$_3$Ti]$^-$. Anal. Calcd for $C_{27}H_{24}O_9TiLi_2 \cdot 2DMF \cdot H_2O$: C, 56.85; H, 6.10; N, 3.68. Found: C, 56.17; H, 5.86; N, 3.98.

Li$_2$[(5d)$_3$Ti]/Li$_4$[(5d)$_6$Ti$_2$]. ^{1}H NMR (methanol-d_4, 300 MHz): monomer (minor component) δ (ppm) = 6.91 (dd, $J = 7.4$, 2.0 Hz, 3 H), 6.38 (m, 6 H), 3.00 (t, $J = 6.9$ Hz, 6 H), 1.45 (m, 6 H); dimer (major component) δ (ppm) = 7.02 (m, 6 H), 6.50 (m, 12 H), 2.64 (m, 6 H),

(45) Perez, H. I.; Luna, H.; Manjarrez, N.; Solis, A.; Nunez, M. A. *Tetrahedron: Asymmetry* **2000**, *11*, 4263−4268.
(46) Wenkwert, E.; Greenberg, R. S.; Kim, H. S. *Helv. Chim. Acta* **1987**, *70*, 2159.
(47) Otwinowski, Z.; Minor, W. *Methods Enzymol.* **1997**, *276*, 307−326.
(48) Sheldrick, G. M. *Acta Crystallogr.* **1990**, *A46*, 467−473.
(49) *Xtal3.7 System*; Hall, S. R., du Boulay, D. J., Olthof-Hazekamp, R., Eds.; University of Western Australia: 2000.

Table 3. Crystallographic Data for $Li[Li_3(\mathbf{4})_6Ti_2]$, $Li[Li_3(\mathbf{5b})_6Ti_2]$, and $Li[Li_3(\mathbf{7a})_6Ti_2]$

compound	$Li[Li_3(\mathbf{4})_6Ti_2]$	$Li[Li_3(\mathbf{5b})_6Ti_2]$	$Li[Li_3(\mathbf{7a})_6Ti_2]$
formula	$Li(C_3H_7NO)_4$-$Li_3[(C_7H_4O_3)_6Ti_2]$	$Li(C_3H_7NO)_4$-$Li_3[(C_9H_8O_3)_6Ti_2]\cdot 2\ C_3H_7NO$	$Li(C_3H_7NO)_2(H_2O)$-$Li_3[(C_7H_4O_3)_6Ti_2]\cdot 2\ C_3H_7NO$
fw	1232.56	1547.05	1430.72
T (K)	198(2)	150	198(2)
wavelength (Å)	0.710 73	1.541 79	0.710 73
crystal system	monoclinic	monoclinic	monoclinic
space group	$P2_1/c$	Cc	$P2_1/c$
a (Å)	16.943(1)	17.845(2)	14.530(1)
b (Å)	23.962(1)	23.754(7)	21.692(1)
c (Å)	14.483(1)	18.033(2)	22.298(1)
α (deg)	90	90	90
β (deg)	97.16(1)	96.43(1)	108.38(1)
γ (deg)	90	90	90
V (Å^3)	5834.1(6)	7596(3)	6669.5(6)
Z	4	4	4
D_{calcd} (Mg m^{-3})	1.403	1.353	1.425
μ (mm^{-1})	0.355	2.459	0.329
F (000)	2544	3248	2968
crystal size (mm^3)	0.50 × 0.20 × 0.20	0.4 × 0.4 × 0.4	0.40 × 0.25 × 0.25
θ range (deg)	1.65−25.00	3.11−73.07	2.14−25.00
reflections coll.	18 701	7589	38 983
independent refl.	10 252	7000	11 730
$R_{(int)}$	0.046	0.083	0.081
data/restr./param.	10 252/0/755	7000/11/684	11 730/8/854
GOF	1.023	1.011	1.024
R [$I > 2\sigma(I)$], R1, wR^2	0.095, 0.259		0.087, 0.229
R (all data), R1, wR^2	0.135, 0.290	0.130, 0.198	0.138, 0.263
max. diff. peak/hole (e Å^{-3})	2.30, −0.58	1.31, −1.32	1.66, −0.75
remarks	cation refined with split positions, occupancy 0.54/0.46(1)	Free solvent molecules and the Li^+ cation plus its four ligands refined as rigid groups with common isotropic displacement parameters. Atoms Li1, Li2, O2c, O3b, C9f, C6e, O3a, and C6f only refined isotropically.	Free solvent molecules refined with common U_{iso} each, one with geom. restraints (SAME)

1.88 (m, 6 H); overlapping signals 1.10−0.6 (m). Negative ESI FTICR-MS (THF): m/z = 1269 $[Li_3(\mathbf{5d})_6Ti_2]^-$, 631 $[Li(\mathbf{5d})_3Ti]^-$. − IR (KBr): ν (cm^{-1}) = 2955, 2926, 1654, 1430, 538.

$Li_2[(\mathbf{5e})_3Ti]/Li_4[(\mathbf{5e})_6Ti_2]$. ^{1}H NMR (methanol-$d_4$, 300 MHz): monomer (minor component): δ (ppm) = 6.91 (dd, J = 7.4, 2.0 Hz, 3 H), 6.38 (m, 6 H), 3.00 (t, J = 7.7 Hz, 6 H), 1.46 (m, 6 H); dimer (major component): δ (ppm) = 7.02 (m, 6 H), 6.50 (m, 12 H), 2.62 (m, 6 H), 1.90 (m, 6 H); overlapping signals: 1.10−0.6 (m). − IR (KBr): ν (cm^{-1}) = 2926, 2860, 1650, 1429, 1257, 1215, 733. − Negative FT-ICR ESI-MS (THF): m/z = 1353.5 $[Li_3(\mathbf{5e})_6Ti_2]^-$, 673 $[Li(\mathbf{5e})_3Ti]^-$. − Calcd. for $C_{36}H_{42}O_9TiLi_2\cdot 3\ H_2O$: C 58.87, H 6.59; found: C 58.39, H 6.33.

$Li_2[(\mathbf{5f})_3Ti]/Li_4[(\mathbf{5f})_6Ti_2]$. ^{1}H NMR (methanol-$d_4$, 400 MHz): (minor component): δ (ppm) = 6.90 (m, 3 H), 6.37 (m, 6 H), 2.98 (t, J = 7.1 Hz, 6 H); dimer (major component): δ (ppm) = 7.01 (m, 6 H), 6.48 (m, 12 H), 2.61 (m, 6 H), 1.89 (m, 6 H), 0.69 (t, J = 7.4, 18 H); overlapping signals: 1.10−0.72 (m). − IR (KBr): ν (cm^{-1}) = 3432, 2924, 1655, 1431, 1259, 1216, 671, 538. − Negative FT-ICR ESI-MS (THF): m/z = 1437.6 $[Li_3(\mathbf{5f})_6Ti_2]^-$, 715 $[Li(\mathbf{5f})_3Ti]^-$. − Calcd. for $C_{39}H_{48}O_9TiLi_2\cdot DMF\cdot 5\ H_2O$: C 56.95, H 7.40, N 1.58; found: C 56.29, H 7.50, N 1.41.

$Li_2[(\mathbf{5\ g})_3Ti]/Li_4[(\mathbf{5\ g})_6Ti_2]$. ^{1}H NMR (methanol-$d_4$, 300 MHz): monomer (minor component) δ (ppm) = 6.98 (m, 3 H), 6.46 (m, 6 H), 3.07 (t, J = 7.5 Hz, 6 H); (major component) δ (ppm) = 7.10 (m, 6 H), 6.59 (m, 12 H), 2.70 (m, 6 H), 1.98 (m, 6 H), 0.82 (t, J = 7.2, 18 H); overlapping signals 1.10−0.72 (m). IR (KBr): ν (cm^{-1}) = 2954, 2924, 1655, 1431, 1258, 1217, 734. Negative ESI FTICR-MS (THF): m/z = 1522 $[Li_3(\mathbf{5g})_6Ti_2]^-$, 757 $[Li(\mathbf{5g})_3Ti]^-$. Anal. Calcd for $C_{39}H_{48}O_9TiLi_2\cdot DMF\cdot 2\ H_2O$: C, 61.86; H, 7.50; N, 1.60. Found: C, 61.96; H, 7.15; N, 1.89.

$Li_2[(\mathbf{5h})_3Ti]/Li_4[(\mathbf{5h})_6Ti_2]$. ^{1}H NMR (methanol-$d_4$, 400 MHz): monomer (minor component) δ (ppm) = 7.00 (dd, J = 8.0, 1.9 Hz, 3 H), 6.44 (m, 6 H), 3.07 (t, J = 7.7 Hz, 6 H); dimer (major component) δ (ppm) = 7.09 (m, 6 H), 6.57 (m, 12 H), 2.70 (m, 6 H), 1.99 (m, 6 H), 0.85 (t, J = 7.1, 18 H); overlapping signals 1.10−0.72 (m). IR (KBr): ν (cm^{-1}) = 2924, 1655, 1432, 1258, 1217. Negative ESI FTICR-MS (THF): m/z = 1606 $[Li_3(\mathbf{5h})_6Ti_2]^-$, 799 $[Li(\mathbf{5h})_3Ti]^-$. Anal. Calcd for $C_{39}H_{48}O_9TiLi_2\cdot 3\ H_2O$: C, 62.79; H, 7.73. Found: C, 62.14; H, 7.12

$Li_2[(\mathbf{5i})_3Ti]/Li_4[(\mathbf{5i})_6Ti_2]$. ^{1}H NMR (methanol-$d_4$, 400 MHz): monomer (minor component) δ (ppm) = 6.99 (dd, J = 8.0, 1.6 Hz, 3 H), 6.48 (dd, J = 8.0, 1.6 Hz, 3 H), 6.43 (t, J = 8.0 Hz, 3 H), 3.08 (t, J = 7.4 Hz, 6 H), 1.56 (m, 6 H); dimer (major component) δ (ppm) = 7.10 (m, 6 H), 6.58 (m, 12 H), 2.70 (m, 6 H), 1.98 (m, 6 H), 0.88 (t, J = 7.1, 18 H); overlapping signals 1.30−0.90 (m). IR (KBr): ν (cm^{-1}) = 2924, 2852, 1655, 1431, 1258, 1217. Negative ESI FTICR-MS (THF): m/z = 1774 $[Li_3(\mathbf{5i})_6Ti_2]^-$, 883 $[Li(\mathbf{5i})_3Ti]^-$. Anal. Calcd for $C_{51}H_{72}O_9TiLi_2\cdot 2\ H_2O$: C, 66.08; H, 8.26. Found: C, 65.67; H, 8.18.

$Li_2[(\mathbf{5j})_3Ti]/Li_4[(\mathbf{5j})_6Ti_2]$. ^{1}H NMR (methanol-$d_4$, 300 MHz): monomer (minor component): δ (ppm) = 7.00 (dd, J = 7.2, 1.7 Hz, 3 H), 6.46 (m, 6 H), 3.08 (t, J = 7.1 Hz, 6 H), 1.57 (m, 2H); dimer (major component) δ (ppm) = 7.09 (dd, J = 6.1, 3.4 Hz, 6 H), 6.58 (m, 12 H), 2.68 (m, 6 H), 1.98 (m, 6 H), 0.89 (t, J = 6.9, 18 H); overlapping signals 1.40−1.00 (m). IR (KBr): ν (cm^{-1}) = 3405, 2924, 2853, 1654, 1432, 1259, 1217. Negative ESI FTICR-MS (THF): m/z = 1942 $[Li_3(\mathbf{5j})_6Ti_2]^-$, 961 $[Li(\mathbf{5j})_3Ti]^-$. Anal. Calcd for $C_{57}H_{84}O_9TiLi_2\cdot {}^1/_4H_2O$: C, 68.24; H, 8.04. Found: C, 69.85; H, 8.69.

$Li_2[(6a)_3Ti]/Li_4[(6a)_6Ti_2]$. ^{1}H NMR (methanol-$d_4$, 400 MHz): monomer (major component) δ (ppm) = 6.95 (dd, J = 7.4, 2.2 Hz, 3 H), 6.44 (m, 6 H), 4.03 (sept, J = 6.9 Hz, 3 H), 1.02 (d, J = 6.9 Hz, 18 H); dimer (traces) δ (ppm) = 0.70 (d, J = 6.5 Hz, 18 H), 0.32 (d, J = 6.5 Hz, 18 H). IR (KBr): ν (cm^{-1}) = 2967, 1655, 1429, 1259, 1217. Negative ESI FTICR-MS (THF): m/z = 1185 $[Li_3(\mathbf{6a})_6Ti_2]^-$, 1179 $[HLi_2(\mathbf{6a})_6Ti_2]^-$, 1173 $[H_2Li(\mathbf{6a})_6Ti_2]^-$, 589 $[Li(\mathbf{6a})_3Ti]^-$, 583 $[H(\mathbf{6a})_3Ti]^-$. Anal. Calcd for $C_{27}H_{24}O_9TiLi_2 \cdot 7\ H_2O \cdot DMF$: C, 49.82; H, 6.46; N, 1.76. Found: C, 49.77; H, 6.76; N, 1.31.

$Li_2[(6b)_3Ti]/Li_4[(6b)_6Ti_2]$. ^{1}H NMR (methanol-$d_4$, 400 MHz): δ (ppm) = 7.73 (m, 6 H), 7.42 (m, 3 H), 7.23 (m, 6 H), 6.70 (m, 3 H), 6.44 (m, 6 H). IR (KBr): ν (cm^{-1}) = 3021, 1631, 1437, 1259, 1217, 766. Negative ESI FTICR-MS (THF): m/z = 1389 $[Li_3(\mathbf{6b})_6Ti_2]^-$, 1383 $[HLi_2(\mathbf{6b})_6Ti_2]^-$, 1377 $[H_2Li(\mathbf{6b})_6Ti_2]^-$, 691 $[Li(\mathbf{6b})_3Ti]^-$, 685 $[H(\mathbf{6b})_3Ti]^-$ (dimer signals are low in intensity).

$Li_2[(7a)_3Ti]/Li_4[(7a)_6Ti_2]$. ^{1}H NMR (DMSO-$d_6$, 400 MHz): monomer (minor component) δ (ppm) = 6.77 (dd, J = 8.0, 1.4 Hz, 3 H), 6.27 (t, J = 8.0 Hz, 3 H), 6.13 (dd, J = 8.0, 1.4 Hz, 3 H), 3.65 (s, 9 H); dimer (major component) δ (ppm) = 6.98 (dd, J = 8.0, 1.7 Hz, 6 H), 6.55 (t, J = 8.0 Hz, 6 H), 6.46 (dd, J = 8.0, 1.7 Hz, 6 H), 2.96 (s, 18 H). Negative ESI FTICR-MS (THF): m/z = 1113 $[Li_3(\mathbf{7a})_6Ti_2]^-$ (no signal for monomer observed). Anal. Calcd for $C_{24}H_{18}O_{12}TiLi_2 \cdot H_2O \cdot 2DMF$: C, 49.74; H, 4.73; N, 3.87. Found: C, 49.97; H, 4.97; N, 3.50.

X-ray Crystallographic Study of $Li_4[Ti_2(7a)_6]$: A data set was collected with a Nonius KappaCCD diffractometer, equipped with a rotating anode generator. Programs used: data collection COLLECT (Nonius B.V., 1998), data reduction Denzo-SMN,[36] structure solution SHELXS-97,[37] structure refinement SHELXL-97 (G. M. Sheldrick, Universität Göttingen, 1997), graphics SCHAKAL (E. Keller, Universität Freiburg, 1997).

$Li_2[(7b)_3Ti]/Li_4[(7b)_6Ti_2]$. ^{1}H NMR (DMSO-$d_6$, 400 MHz): monomer (minor component) δ (ppm) = 6.76 (dd, J = 8.2, 1.7 Hz, 3 H), 6.26 (t, J = 8.2 Hz, 3 H), 6.12 (dd, J = 8.2, 1.7 Hz, 3 H), 4.12 (q, J = 7.1 Hz, 6 H), 1.22 (t, J = 7.1 Hz, 9 H); dimer (major component) δ (ppm) = 6.97 (dd, J = 8.2, 1.6 Hz, 6 H), 6.52 (t, J = 8.2 Hz, 6 H), 6.43 (dd, J = 8.2, 1.6 Hz, 6 H), 3.50 (m, 6 H), 3.03 (m, 6 H), 0.95 (t, J = 7.1 Hz, 18 H). Negative ESI FTICR-MS (THF): m/z = 1197 $[Li_3(\mathbf{7b})_6Ti_2]^-$ (no signal for monomer observed). Anal. Calcd for $C_{27}H_{24}O_{12}TiLi_2 \cdot H_2O \cdot DMF$: C, 51.97; H, 4.80; N, 2.02. Found: C, 52.26; H, 5.18; N, 2.23.

Acknowledgment. Funding from the Deutsche Forschungsgemeinschaft (inter alia SFB 624) and the Fonds der Chemischen Industrie is acknowledged. C.A.S. thanks the DFG for a Heisenberg fellowship and the FCI for a Dozentenstipendium.

Supporting Information Available: ORTEP Plots of the X-ray structures of $[Li_3(\mathbf{4})_6Ti_2]^-$, $[Li_3(\mathbf{5b})_6Ti_2]^-$, and $[Li_3(\mathbf{7a})_6Ti_2]^-$ and X-ray crystallographic files (three CIF files). This material is available free of charge via the Internet at http://pubs.acs.org.

JA052326J